

32 Abstract

33

34 This study evaluated microbial systems and technological approaches to configure the whole
35 slurry co-fermentation process for ethanol biosynthesis from a novel stover system rich in high
36 sugars. Two approaches, namely separate and simultaneous hydrolysis and co-fermentation
37 (SHCF and SSCF, respectively), were investigated using *Escherichia coli* monoculture and *E. coli*-
38 yeast coculture. The SSCF with *E. coli* monoculture produced 32.75 g/L ethanol, representing only
39 44.87% yield, which left 65.13 g/L of total sugars unconverted and exhibited limited xylose
40 consumption. Subsequently, a coculture-based SHCF significantly enhanced sugar consumption,
41 leading to increases in both ethanol yield and concentration to 66.94% and 48.86 g/L, respectively.
42 Nevertheless, xylose utilization remained minimal due to the preference for glucose and the
43 inhibitory effects of certain compounds. Thereafter, modification of the medium composition by
44 supplementing betaine and sodium metabisulfite improved ethanol production to 53.18 g/L by
45 reducing the toxic effects of inhibitors. Finally, a dual-phase SSCF (DP-SSCF) was explored by
46 allowing the consumption of sugars from the pretreated slurry in the first phase, followed by
47 concurrent cellulose hydrolysis and utilization of the resulting glucose in the second phase. This
48 strategy increased ethanol titer to 63.14 g/L, with 84.3% yield and 0.88 g/L/h productivity.

49

50 **Keywords:** Corn stover; Bioethanol; Microbial coculture; Biorefinery; Bioprocessing.

51

52 1. Introduction

53

54 Rising concerns over the energy crisis and the ecological impacts of burning fossil fuels have
55 driven substantial research into biofuels in the past two decades. Among biofuels, bioethanol holds
56 promise as an eco-friendly alternative to traditional fuels because of its capacity to lessen
57 greenhouse gas release, serve as a cleaner gasoline additive, and be produced from inexpensive
58 and renewable resources (Malik et al., 2022). Studies indicate that bioethanol emits 39-43% less
59 greenhouse gases than gasoline, the value could be even higher up to 47-70% (Jarunglumlert and
60 Prommuak, 2021; Lewandrowski et al., 2020). In 2020, the international bioethanol industry was
61 worth approximately US\$ 58.44 billion, and it is estimated to climb to US\$ 64.8 billion by 2028
62 (Zabed et al., 2023b). Beyond its role as a biofuel, ethanol finds extensive use in alcoholic

63 beverages, pharmaceuticals, healthcare, and cosmetics. Recognizing its versatile applications,
64 ethanol is listed among the top 10 valuable biobased materials (Bozell and Petersen, 2010).

65
66 Ethanol can be generated through the conversion of various biomass resources, primarily rich
67 in carbohydrates, including starch, sugar, lignocellulosic waste, and algae (Periyasamy et al., 2023;
68 Zabed et al., 2019). Among them, lignocellulose-based wastes, especially agro-waste, hold more
69 promise because it is abundantly available from non-food sources without requiring any direct land
70 usage. Nevertheless, lignocellulosic ethanol has some techno-economic obstacles stemming from
71 the intricate biomass structure (Hilares et al., 2022; Rathour et al., 2023). Consequently, despite
72 significant policy decisions and financial support over the past decade, ethanol generation from
73 lignocellulose-based biomass remains at a nascent stage. Within the realm of agro-based wastes,
74 corn stover is the largest with its excellent holocellulose content (He et al., 2023; Ntakirutimana
75 et al., 2023). It is attainable after the main crop (grain) is harvested, with around 47–50% of the
76 dry mass of the total kernel yield (Wojcieszak et al., 2020). The estimated global stover yield
77 amounts to a staggering 1661.25 million tons annually (Wang et al., 2020), making up 27.2% of
78 the world's total agro-waste (Noppawan et al., 2021).

79
80 Over the past years, there has been extensive research into the use of stover for ethanol
81 production (Peng et al., 2023; Zabed et al., 2023b). Despite these efforts, the economic feasibility
82 of stover-based ethanol remains questionable, which stems from the high processing costs, and
83 low yields of recovered sugars and ethanol (Zhang et al., 2023). One strategy to enhance the overall
84 feasibility of this conversion process is to make integrated use of both soluble and insoluble
85 carbohydrates of stovers. This is crucial because the incomplete conversion of the fermentable
86 components in stover leads to diminished ethanol yields. However, the predominant practice in
87 current stover-based ethanol production primarily focuses on converting cellulose and/or
88 hemicellulose, often disregarding soluble sugar fraction. Furthermore, normal corn stover contains
89 low levels of sugars, making their extraction economically unviable. While increasing the solid
90 content could theoretically boost ethanol yields, it has some inherent limitations and necessitates
91 additional enzyme usage (da Silva et al., 2020; Reis et al., 2023). Consequently, there remains a
92 pressing need for sustainable and innovative technologies to enhance stover-to-ethanol conversion.

93

94 An alternative solution that could potentially improve ethanol yield without incurring extra
95 enzyme costs involves utilizing sugary stover derived from sweet corn, which possesses a higher
96 sugar content compared to normal stover (Barros-Rios et al., 2015). However, sweet corn is
97 primarily cultivated for its grain as a food source, and hence, maintaining a balance between sugar
98 content in its grain and stover poses a significant challenge (Santos et al., 2014). Additionally,
99 sugar content in both stover and grains diminishes over time during various stages of plant growth.
100 Given these points, novel corn hybrids with high sugar content were reported with the ability to
101 grow in conditions akin to those of normal maize varieties (Zabed et al., 2016a). These specialized
102 corn varieties yield high-sugary stover (HSS) rich in soluble sugars at their early growth stages,
103 particularly at the dough stage, called R4 stage (Akter et al., 2020). This new stover system could
104 serve as a compelling addition to current stover-based ethanol.

105
106 In response to the aforementioned techno-economic concerns, there is a recent shift towards
107 adopting whole slurry fermentation over the traditional solid/liquid separation method aiming to
108 minimize both time and energy consumption (Bukhari et al., 2021). The conventional solid/liquid
109 separation process is considered techno-economically less viable due to its additional water usage,
110 energy input, and wastewater generation (Singh et al., 2021). Due to its advantages, the whole-
111 slurry-based approach is gaining significance in ethanol production from biomass. For example,
112 this technology has been applied to auto-hydrolyzed stover with varying concentrations of washed
113 liquid, which provided an impressive 80% ethanol conversion yield (del Río et al., 2020).
114 Furthermore, this strategy is equally applicable to the two widely used ethanol production
115 technologies from mixed sugars, namely separate and simultaneous hydrolysis and co-
116 fermentation, known as SHCF and SSCF, respectively (Zabed et al., 2023b; Zhang et al., 2022).
117 However, this approach is relatively new when dealing with sugary stovers, demanding a careful
118 configuration to achieve efficient ethanol generation from this stover type.

119
120 One of the primary challenges to ethanol production from sugary stovers using the whole-
121 slurry-based technique, particularly during SHCF, would be the negative effects of glucose or other
122 soluble sugars on cellulose hydrolysis above a certain level of total sugars. This leads to a glucose
123 yield from cellulose that falls short of the theoretical maximum. In this context, the use of SSCF
124 technology could be explored, which is considered to be more promising in terms of efficiency

125 and yield (Zabed et al., 2023b; Zhu et al., 2020). This technology has been gaining prominence in
126 ethanol production due to several advantages over its counterpart SHCF, including lower costs,
127 shorter time, higher solid load, lower risk of contamination, and higher ethanol yield (Liu et al.,
128 2019). SSCF is further important to prevent the inhibitory effects of glucose on cellulases,
129 especially during high-solid load fermentation when glucose can act as an end-product inhibitor
130 of the enzymes (del Río et al., 2020).

131

132 While SSCF appears promising as an attractive alternative to SHCF for the co-fermentation of
133 mixed sugars obtained from HSS, a further question may arise whether the commonly used single-
134 phase SSCF can overcome the effects of initial sugars present in the pretreated slurries on cellulose
135 hydrolysis. Because sugary stovers can also add fructose and sucrose or the hydrolysis products of
136 sucrose (fructose and glucose) in addition to the common sugars from stover (Akter et al., 2020;
137 Barros-Rios et al., 2015). Furthermore, single-phase SSCF faces a limitation with the most
138 commonly used yeast strain, *S. cerevisiae*, since wild yeast strains lack the metabolic pathways
139 required to convert pentose sugars unless they undergo significant metabolic modification.
140 Another commonly employed bacterial strain, *E. coli* KO11, can ferment both pentose and hexose
141 sugars. However, its preference for glucose may result in an inefficient conversion rate of other
142 sugars until glucose depletes or reaches a certain level, which would be challenging as cellulose
143 hydrolysis continues. Given these considerations, reconfiguration of SSCF is important for ethanol
144 production from HSS, in which double-phase SSCF (DP-SSCF) could be an attractive option. In
145 this approach, initial sugars present in pretreated slurries could be consumed by *E. coli*, followed
146 by the addition of cellulose-degrading enzymes and yeast in the 2nd phase.

147

148 This study aimed at configuring a suitable co-fermentation technology for ethanol production
149 from HSS by evaluating microbial systems and process configurations. In this context, HSS
150 obtained from a high sugar-containing maize variety (named UM.NF-6) was studied after
151 harvesting it at the R4 stage, as detailed earlier (Zabed et al., 2023a). The collected stovers were
152 investigated during SHCF or SSCF technologies in various configurations using previously
153 evolved *S. cerevisiae* and *E. coli* in monoculture or co-culture systems. Initially, SHCF was
154 conducted by subjecting the whole-slurry hydrolysate to fermentation without prior detoxification
155 using *E. coli* monoculture. Subsequently, a systematic study was done to investigate the effects of

156 additives and inhibitors present in the hydrolysate on microbial growth and fermentation
157 efficiency, together with the necessary process configuration. Finally, ethanol production was
158 investigated using the DP-SSCF. The findings of this study could open a new dimension in
159 lignocellulosic biorefinery to improve its viability by introducing sugary biomass or integrating
160 agro-wastes with sugary wastes such as molasses to achieve a high titer of the desired product.

161

162 **2. Materials and methods**

163

164 2.1. Materials

165

166 The HSS was collected from a maize variety (named UM.NF-6) grown in the field of the
167 University of Malaya (Kuala Lumpur, Malaysia) (Zabed et al., 2023a). It was harvested during the
168 R4 (dough) stage because this stage offers the highest sugar content (Akter et al., 2020; Zabed et
169 al., 2023a). The stover samples were subsequently oven-dried (at 70°C) until their water level
170 reached approximately 12%, after which they were ground to a particle size of less than 1.0 mm.
171 The methods for growing the corn plants, managing them, and harvesting and processing the HSS
172 were similar to those previously described (Akter et al., 2020; Zabed et al., 2016a), with the only
173 difference being that the cropping year for this study was 2019. The composition of the HSS is as
174 follows (in % dry matter): total sugars [(27.18; containing sucrose (12.59), glucose (7.7), and
175 fructose (6.89)], cellulose (28.54), hemicellulose (16.51), and lignin (8.57). Yeast extract peptone
176 dextrose (YPD) broth composed of (in g/L) yeast extract (10), peptone (20), and glucose (20);
177 YPD agar contained YPD broth and 15 g/L agar; Luria Broth (LB) broth consisted of (in g/L)
178 tryptone (10), yeast extract (5), and NaCl (10); and LB agar composed of LB broth with 15 g/L
179 agar. These materials were obtained from BD Difco Biosciences (Franklin Lakes, NJ). Activated
180 carbon [CAS# 64365-11-3; internally porous microcrystalline structure and non-graphitic form of
181 carbon; modified with Bis(2-ethylhexyl)phosphate] was purchased from Aladdin (Shanghai,
182 China). Other chemicals, reagents, and standards were sourced from Sigma-Aldrich (Beijing,
183 China), or Aladdin.

184

185

186 2.2. Enzymes and microorganisms

187
188 Celluclast 1.5L (a cellulase enzyme, with an activity level of ≥ 700 U/g), Novozyme 188 (a β -
189 glucosidase enzyme with an activity level of ≥ 250 U/g), and xylanase (with an activity level of
190 ≥ 2500 U/g) were sourced from Sigma-Aldrich. The *S. cerevisiae* and *E. coli* strains employed in
191 this research were maintained in our laboratory. Initially, both strains were procured from the
192 ATCC (Manassas, VA, USA) as *S. cerevisiae* 96581 and *E. coli* KO11 55124, respectively, which
193 were previously evolved by iterative exposure to the acid-pretreated biomass liquor to improve
194 their tolerance to inhibitors. *S. cerevisiae* strain was cultured on YPD agar (30°C and 48 h),
195 followed by transferring to YPD liquid medium and incubating at 30°C with constant agitation at
196 200 rpm for 24 h. Aliquots were preserved with 30% glycerol at -80°C for future use. *E. coli* strain
197 was cultivated on LB agar at 37°C for 24 h, followed by transfer to LB broth and overnight growth
198 at 37°C with continuous shaking at 200 rpm.

199 200 2.3. Processing of stovers to prepare pretreated slurry and hydrolysate for fermentation

201
202 To prepare whole pretreated slurry, dilute-acid pretreatment was done under the optimum
203 conditions established earlier in our laboratory (Zabed et al., 2023a), with a slight modification by
204 the addition of 2% syringic acid as discussed earlier (Zhai et al., 2018). The purpose of adding
205 syringic acid (a carbocation agent) during pretreatment was to reduce the effects of phenolic
206 inhibitors on subsequent cellulose hydrolysis, as reported before (Zhai et al., 2018). Briefly, 100
207 ml of 20% slurry of HSS was prepared in 0.5% H₂SO₄ solution containing 2% SA. The entire
208 mixture was then placed into an autoclave reactor made of stainless-steel (Model: KH-400ml,
209 Yushen, Shanghai, China), which was positioned on a sand bath. The pretreatment process was
210 carried out at a temperature of 155 °C for 30 min by continuously stirring the content with a turbine
211 impeller at a speed of 200 rpm (Zabed et al., 2023a). After pretreatment, the container was taken
212 out of the heated sand and brought to room temperature using chilled water. The resulting whole
213 pretreated slurry was subsequently subjected to saccharification with enzymes.

214
215 Saccharification was performed in a fed-batch system using the modified method discussed
216 earlier (Gao et al., 2014). The conditions used in saccharification were previously configured and

217 optimized for sugary stovers in our lab (unpublished work). Briefly, the pretreated stover slurry
218 was pH adjusted to 4.8 with an ammonia solution (28%, w/w) (Moxley et al., 2012) and then
219 supplemented with 0.4% polyethylene glycol (Singh et al., 2021). The slurry was buffered with
220 Na acetate-acetic acid buffer to 0.075 M as the final concentration (Moxley et al., 2012).
221 Thereafter, half of the slurry was transferred to a 250 mL flask, followed by adding half of the
222 optimum enzyme cocktail to it at 0 h of hydrolysis. The enzyme cocktail was previously optimized
223 in our lab (unpublished work), which consisted of 20 mg/g glucan of Celluclast 1.5L (equivalent
224 to 14 U/g glucan), 10 mg/g glucan of Novozyme 188 (equivalent to 2.5 U/g glucan), and 10
225 mg/g glucan xylanase (equivalent to 25 U/g glucan). The remaining enzymes and slurry were fed in
226 two equal feeds after 12 h and 24 h. The hydrolysis was continued until 72 h in an orbital shaker
227 at 50 °C and 150 rpm (Zabed et al., 2023a). To prevent experimental errors, a blank was maintained
228 using water in place of the stover sample, with all other supplements and process conditions kept
229 the same.

230

231 2.4. Seed culture preparation for fermentation

232

233 To prepare the seed culture of *S. cerevisiae*, the preserved culture was first grown on YPD agar
234 at 30 °C for a duration of 48 h (Akter et al., 2020). Subsequently, single colonies were transferred
235 into 100 ml of YPD broth in 250 ml Erlenmeyer flasks. The culture was allowed to grow for 18 h
236 at 30°C and then used as inoculum or seed culture for fermentation. In a similar manner, the seed
237 culture of *E. coli* was prepared by cultivating the preserved culture on LB agar at 37°C for 24 h
238 (Akter et al., 2020). Afterward, individual colonies were transferred into LB broth and cultured
239 overnight at 37°C to obtain the respective inoculum or seed culture.

240

241 2.5. Co-fermentation of hydrolysate using *E. coli* monoculture and *E. coli*-yeast coculture

242

243 In 250 Erlenmeyer flasks, 100 ml of hydrolysate was taken and supplemented with yeast
244 extract (5 g/L), tryptone (10 g/L), and NaCl (10 g/L) (Akter et al., 2020), following the composition
245 of LB broth for both *E. coli* and *S. cerevisiae* strains, as discussed earlier (Li et al., 2010). For
246 monoculture-based co-fermentation with *E. coli*, the pH was set to 7.0, followed by adding seed
247 culture at a concentration of 3×10^6 colony-forming-unit (CFU)/ml, equivalent to 6.48 log₁₀

248 CFU/ml (Akter et al., 2020). Fermentation took place in an incubator shaker at 37°C and 150 rpm
249 for 120 h (Akter et al., 2020). In the case of co-fermentation using *E. coli*-*S. cerevisiae* coculture
250 system, the pH was maintained at 6.0, and the temperature was kept at 35°C (Li et al., 2010).
251 Inoculation involved 3×10⁶ CFU/ml of *E. coli* (equivalent to 6.48 log₁₀ CFU/ml) and 1×10⁶
252 CFU/ml of *S. cerevisiae* (equivalent to 6 log₁₀ CFU/ml) seed culture at a ratio of 3:1 (based on
253 preliminary trial). Samples were regularly withdrawn for microbial count and the analysis of
254 sugars and metabolites. To prevent experimental errors, a blank was maintained using water in
255 place of the stover sample, with all other supplements and process conditions kept the same. The
256 theoretical ethanol yield was calculated using Eq. (1) based on the released sugars present in the
257 hydrolysates.

$$258 \quad \text{Ethanol yield (\%)} = \frac{\text{Ethanol produced (g/L)}}{[0.51 \times \text{Total sugars (g/L)}]} \times 100\% \quad (1)$$

259
260 where, 0.51 (g/g) is the theoretical ethanol yield from monosaccharides (glucose, xylose, and
261 fructose). Despite 0.54 (g/g) being the theoretical ethanol yield from sucrose, it was not considered
262 in this study due to its insignificant amount in the hydrolysate as well as the difficulties of
263 measuring ethanol production separately from sucrose under the co-fermentation conditions.

264 265 2.6. Effects of additives and inhibitors on co-fermentation 266

267 To determine the possible effects of additives (syringic acid added during pretreatment and
268 polyethylene glycol added during saccharification) on co-fermentation, hydrolysates were
269 prepared according to the methods discussed in Section 2.3 with the required modification as
270 follows: syringic acid was not used during pretreatment, while the resulting pretreated slurry was
271 subjected to saccharification without the addition of polyethylene glycol. In this way, a modified
272 hydrolysate was obtained. Thereafter, one set of this modified hydrolysate was detoxified to
273 remove or reduce inhibitors using the activated carbon method, as discussed earlier (Jung et al.,
274 2013). Briefly, the hydrolysate was first filtered using a cloth to detach liquid and solid portions.
275 Subsequently, 10% (w/v) of powdered activated carbon was added to the liquid part, followed by
276 thorough mixing and stirring at 30°C and 200 rpm for 60 min (Jung et al., 2013). After
277 detoxification, the mixture was subjected to centrifugation (12,000×g, 5 min, 4 °C) to separate

278 activated carbon from the liquid, and the resulting supernatant was reintroduced to the solid
279 fraction separated initially from the pretreated stover slurry. Using the same method, a set of
280 original hydrolysates obtained from additive supplementation (Section 2.3) was also detoxified to
281 compare the results. Thereafter, co-fermentation was performed for the hydrolysate following the
282 same methods used for coculture-based co-fermentation, as discussed in Section 2.5. The results
283 were compared with those obtained from co-fermentation of original hydrolysate (containing
284 additives) under undetoxified conditions by *E. coli*-yeast coculture. To prevent experimental
285 errors, a blank was maintained in each experiment using water in place of the stover sample, with
286 all other supplements and process conditions kept the same.

287

288 2.7. Supplementation of hydrolysate with betaine and sodium metabisulfite

289

290 To minimize the requirement for a separate detoxification step (to reduce the effect of
291 inhibitors), an alternative strategy was applied by mixing the undetoxified hydrolysate (produced
292 under the supplementation with additives, as discussed in Section 2.3) with 1.0 mM betaine and
293 2.6 mM sodium metabisulfite following the methods discussed earlier (Wang et al., 2019).
294 Thereafter, co-fermentation was performed following the same methods used for coculture-based
295 co-fermentation discussed in Section 2.5. The results were compared with those obtained from the
296 co-fermentation of detoxified hydrolysate under similar conditions (using coculture).

297

298 2.8. Double phase SSCF (DP-SSCF) of whole-pretreated slurry

299

300 For the DP-SSCF process, pretreated stover slurry was prepared (Section 2.3) and pH was
301 adjusted to the target pH with ammonia solution. The mixture was supplemented with 0.4%
302 polyethylene glycol and buffered with sodium acetate-acetic acid buffer to 0.075 M as the final
303 concentration (Moxley et al., 2012). The DP-SSCF was configured in two ways: In the first
304 configuration, referred to as DP-SSCF-E/S, *E. coli* and yeast were employed separately in the first
305 and second phases, respectively. In this setup, the optimal pH and temperature were maintained
306 for each strain at 7 and 37°C for *E. coli* and 5 and 30°C for yeast, respectively (Akter et al., 2020).
307 Another configuration, referred to as DP-SSCF-ES/S, involved a coculture system in the first phase
308 to promote the consumption of initial sugars of pretreated slurry, while yeast was employed in the

309 second phase to efficiently utilize cellulose-derived glucose. For this configuration, a pH of 6 and
310 a temperature of 35°C were maintained in the first phase, while the pH and temperature in the
311 second phase were 5 and 30°C, respectively (based on preliminary trial). In DP-SSCF-E/S, the
312 first phase commenced with the addition of *E. coli* monoculture at a concentration of 3×10^6
313 CFU/ml (equivalent to 6.48 log₁₀ CFU/ml) and two-thirds of the nutrients from the medium used
314 in Section 2.5. After 60 h, the second phase was started by adding an enzyme cocktail (comprising
315 20, 10, and 10 mg/g glucan of Celluclast 1.5L, Novozyme 188, and xylanase, respectively), yeast
316 at a concentration of 1×10^6 CFU/ml (equivalent to 6 log₁₀ CFU/ml), and the remaining one-third
317 of the nutrients. Similarly, in DP-SSCF-ES/S, the first phase was started with *E. coli* and *S.*
318 *cerevisiae* at concentrations of 3×10^6 CFU/ml (equivalent to 6.48 log₁₀ CFU/ml) and 5×10^5
319 CFU/ml (equivalent to 5.7 log₁₀ CFU/ml), respectively. The second phase followed the same
320 procedure as DP-SSCF-E/S, with the exception that a yeast inoculum of 5×10^5 CFU/ml (equivalent
321 to 5.7 log₁₀ CFU/ml) was used. The entire SSCF process took 120 h to complete, with samples
322 being withdrawn every 24 h to analyze biomass, metabolites and sugars. To prevent experimental
323 errors, a blank was maintained in each experiment using water in place of the stover sample, with
324 all other supplements and process conditions kept the same. The theoretical ethanol yield was
325 calculated using Eq. (1) considering the total released sugars, which consisted of soluble sugars
326 present in the pretreated slurry and sugars that could theoretically be released from cellulose and
327 residual hemicellulose of the pretreated slurry. The overall workflow of this study is shown in Fig.
328 1.

329

330 2.9. Analytical methods

331

332 Bacterial and yeast counts were determined by the indirect plate-count method, utilizing the
333 collected samples without undergoing centrifugation and the results were expressed CFU/ml
334 (Zabed et al., 2016b). In brief, 100 μL of the appropriately diluted fermented sample was
335 introduced into LB agar containing 5 μg of cycloheximide to inhibit yeast growth, followed by
336 incubation of the plate at 37 °C for 24 h (Zabed et al., 2016b). To enumerate yeast cells, 100 μL
337 of the suitably diluted fermented sample was inoculated into YPD agar supplemented with 50
338 μL/ml of chloramphenicol and 50 μL/ml of kanamycin to prevent bacterial proliferation (Zabed et
339 al., 2016b). These plates were then incubated at 30 °C for 48 h (Qin et al., 2017). The microbial

340 counts were expressed as log₁₀ CFU/ml. Soluble sugars in the pretreated slurry or hydrolysate and
341 metabolites in the fermentation broth (supernatant obtained from centrifugation of the collected
342 samples) were quantified utilizing an HPLC system (2030 Plus, Shimadzu, Japan). This system
343 was equipped with a RID (RID 20A, Shimadzu, Japan) and an Aminex HPX-87P column (300
344 ×7.8 mm, BioRad, Hercules, CA). The column temperature was 80 °C, and water was used as the
345 mobile phase, delivered at a flow rate of 0.6 mL/min (Zabed et al., 2023a). Amounts of inhibitors
346 (furfural, 5-hydroxymethylfurfural, and acetic acid) were analyzed in HPLC under the same
347 systems except for that column was 300 ×7.8 mm Aminex HPX-87H column with a column
348 temperature of 65°C and a mobile phase of 0.005 M H₂SO₄ with a flow rate of 0.8 mL/min (Li et
349 al., 2017). The total phenol content was determined by the Folin-Ciocalteu method, with gallic
350 acid serving as the standard (Müller et al., 2010).

351

352 2.10. Statistical analysis

353

354 To examine the variations among the various treatments, a one-way analysis of variance was
355 utilized. Following this, multiple comparisons were executed using the Tukey post-hoc
356 examination. In situations where a comparison between two factors was necessary, the student's t-
357 test was performed. All statistical evaluations were carried out with a 95% confidence level
358 (P<0.05) utilizing Minitab statistical software (16 v., State College, PA) (Zabed et al., 2023a).

359

360 **Fig. 1.**

361

362 **3. Results and discussions**

363

364 3.1. Co-fermentation of undetoxified hydrolysate (SHCF) by *E. coli* monoculture

365

366 The hydrolysate slurry served as the initial material for co-fermentation in this study. It was
367 prepared through the pretreatment and saccharification of HSS, following the methods established
368 before as outlined in Section 2.3. In particular, a carbocation agent (2% syringic acid) was used
369 during pretreatment, which was reported to mitigate the effects of phenolic inhibitors on
370 subsequent cellulose hydrolysis (Zhai et al., 2018). Similarly, as reported earlier (Kim et al., 2019)

371 and we optimized before (unpublished work), a surfactant (0.6% polyethylene glycol) was
372 incorporated into the pretreated slurry during saccharification to minimize unproductive binding
373 between insoluble lignin and enzymes. The compositions of pretreated stover slurry and
374 hydrolysate slurry are summarized in Table 1. Both slurry types contained significant amounts of
375 glucose, fructose, and xylose, corresponding to the intrinsic free sugars and holocellulose contents
376 of the stovers (Section 2.1). Furthermore, the composition of pretreated slurry differed from that
377 mentioned earlier for a similar 20% solid loading (Zabed et al., 2023a), showing an increase in
378 sugar levels and a decrease in inhibitor concentrations. These positive changes could be attributed
379 to the effects of the carbocation agent used in this study. With an average titer of total sugars of
380 83.19 g/L, the pretreated slurry contained 31.26 g/L glucose, mostly derived from the intrinsic
381 glucose content of the stover and hydrolysis of sucrose (another intrinsic sugar) under the
382 pretreatment conditions. Due to cellulose saccharification, glucose concentration increased to
383 86.67 g/L in the hydrolysate, with the total sugar titer reaching 143.12 g/L. The second-highest
384 sugar in the hydrolysate was xylose (24.21 g/L), mainly derived from hemicellulose breakdown
385 during pretreatment, with a further slight increase to 29.59 g/L after hydrolysis due to the
386 breakdown of residual hemicellulose by the added hemicellulase enzymes. With a fructose content
387 of 20.18 g/L in the hydrolysate, this sugar did not exhibit a significant change from that found in
388 the pretreated stover slurry. As explained earlier (Zabed et al., 2023a), the unusually significant
389 presence of fructose in the pretreated stover slurry as well as hydrolysate was due to the intrinsic
390 fructose content of the stover and the hydrolysis of sucrose. In addition to sugars, major inhibitors
391 did not vary significantly between pretreated slurry and hydrolysate ($P>0.05$), as inhibitors are
392 mainly generated during pretreatment (Wang et al., 2018).

393

394 **Table 1**

395

396 To investigate ethanol production, the hydrolysate slurry was subjected to co-fermentation
397 using the monoculture of a previously evolved strain of *E. coli* KO11. This commonly used
398 bacterial strain can ferment mixed sugars containing both pentose and hexose sugars, despite the
399 uptake and metabolism of pentose sugars by this strain being slow at the initial stages due to its
400 glucose preference issue (Aggarwal et al., 2022). As illustrated in Fig. 2a, an apparent lag phase
401 was observed until 3 h during fermentation with *E. coli* monoculture, with cell count rising

402 insignificantly from 6.48 log₁₀ CFU/ml to 6.49 log₁₀ CFU/ml. This duration was slightly
403 lengthier compared to a previously reported lag phase of less than 2 h for an engineered *E. coli*
404 strain utilized in the co-fermentation of xylose and glucose (Fernández-Sandoval et al., 2019). This
405 comparatively extended lag phase might be attributed to the cumulative impact of the harsh
406 conditions of the hydrolysate, particularly stemming from the inhibitors and high concentrations
407 of sugars. Subsequently, an exponential growth phase was observed between 6 h and 12 h,
408 witnessing a surge in cell count from 6.62 log₁₀ CFU/ml to 6.73 log₁₀ CFU/ml (Fig. 2a). The cell
409 count continued to increase until 18 h with a total count of 6.76 log₁₀ CFU/ml, and thereafter cells
410 entered a stationary phase. The stationary phase persisted until 72 h, followed by a decline phase
411 presumably caused by similar factors mentioned for the delayed lag phase. The entry of cells into
412 the death phase after 72 h indicates that there might be toxic effects of either inhibitors or total
413 sugars, even though the strain was evolved before, which might be due to a change in biomass and
414 processing conditions.

415
416 Corresponding to the cell growth, ethanol production remained minimal during the initial
417 3 h, then exhibited an exponential rise until 48 h. With a gradual increase subsequently, the ethanol
418 titer reached 30.59 g/L after 72 h (Fig. 2b). Thereafter, with a slight increase, the ethanol titer
419 reached 32.62 g/L after 96 h and remained almost the same after 120 h. These results indicated an
420 exponential production pattern of ethanol during the logarithmic growth phase, persisting the same
421 pattern until the early stationary phase of the cell growth. While not exhibiting exponential growth,
422 ethanol production continued to rise during the subsequent stationary phase and then followed a
423 cessation in ethanol production as the cells entered into the death phase. These findings align with
424 those reported in a prior study, which also observed a similar pattern in ethanol production, *i.e.*,
425 the maximum ethanol production occurred during the log phase to the early stationary phase
426 (Wang et al., 2019). Accordingly, the productivity of ethanol showed an increase from 0.62 g/L/h
427 after 6 h and peaked at 0.68 g/L/h after 24 h (Fig. 2b). Subsequently, there was a significant
428 decrease in productivity, reaching 0.34 g/L/h after 96 h and 0.27 g/L/h after 120 h. The theoretical
429 ethanol yield exhibited a continual and significant ($P < 0.05$) rise until 96 h from 5.12% after 6 h to
430 44.69% after 96 h (Fig. 2b). Despite a significantly higher total sugar content in the hydrolysate,
431 the achieved ethanol titer was considerably lower in comparison to that reported in the literature.
432 For example, 48.6 g/L ethanol with 0.45 g/g yield (~88% theoretical yield) was reported for

433 lignocellulosic biomass using 20% solid (Wang et al., 2019).

434

435 The consumption of three major sugars (glucose, xylose, and fructose) during fermentation
436 exhibited significant temporal variations. Notably, the consumption of xylose was consistently
437 sluggish throughout the fermentation, leaving 24.1 g/L unconverted (Fig. 2c). In fact, it is a
438 common phenomenon that xylose utilization by microbial cells is affected by glucose during the
439 co-fermentation of both sugars until the glucose levels drop to a critical limit (Dev et al., 2022).
440 Even, a considerable amount of glucose remained unconverted after fermentation, which was more
441 than 43 g/L after 18 h, and dropped to 29.58 g/L after 24 h. For the subsequent time, glucose was
442 consumed slowly, leaving 22.16 g/L unconverted after fermentation (Fig. 2c). As a result, xylose
443 consumption was not seen until 72 h when a small amount of xylose was consumed. Nevertheless,
444 due to the cells entering a decline phase, the consumption of xylose was further curtailed, leading
445 to a major portion of xylose remaining unused (Fig. 2c). Similarly, fructose consumption was also
446 impeded by the co-presence of glucose, albeit exhibiting a drop in fructose levels after 24 h. During
447 this time, fructose consumption surpassed xylose utilization, indicating that the optimal
448 consumption rate of xylose is contingent upon the attaining of critical glucose and fructose
449 thresholds. Nevertheless, a major portion of fructose, 12.87 g/L, was still left unconsumed after
450 fermentation (Fig. 2c). This overall disruption in sugar utilization during fermentation ultimately
451 culminated in a notable accumulation of residual total sugars, totaling 65.13 g/L (Fig. 2c).

452

453 A lower ethanol yield was further caused by the production of unwanted metabolites like
454 lactate, acetate, glycerol, and formate through the central pathway, which all together also
455 consumed a considerable amount of sugars (Lau et al., 2010). However, the formation of these
456 byproducts is an inevitable consequence of cellular metabolic activities through their central
457 pathway, unless the strains are metabolically rewired to prevent their generation (Ko et al., 2020).
458 Since the hydrolysate initially contained 3.73 g/L acetate (Table 1), this amount further increased
459 during fermentation due to the metabolic activity of cells, reaching a peak of 5.33 g/L after 48 h,
460 thus becoming the dominant byproduct (Fig. 2d). Interestingly, a slight decline in acetate was
461 observed after 72 h, suggesting that the cells attempted to utilize this byproduct as a carbon source
462 during the stress-laden late stationary phase or before entering the decline phase. Despite its peak
463 production during fermentation, lactate emerged as the second most abundant unwanted metabolite

464 after acetate. It exhibited a consistent increase from 0.08 g/L after 3 h to 2.68 g/L at the end of
465 fermentation (Fig. 2d). Another metabolite, namely formate, was also detected as the unwanted
466 metabolite during fermentation with *E. coli*, which showed a continuous increase throughout the
467 fermentation from 0.12 g/L to 0.86 g/L as the fermentation period increased from 6 h to 120 h.
468 However, some increases were not statistically significant if compared between two or more
469 sequential periods ($P>0.05$). Considering these findings, especially the sugar consumption and
470 ethanol yield, a monoculture system might not be the optimal choice for fermenting mixed sugars
471 derived from HSS.

472

473 **Fig. 2**

474

475 3.2. Co-fermentation of undetoxified hydrolysate (SHCF) by *E. coli*-yeast coculture

476

477 3.2.1. Preliminary modulation of the coculture system

478 Based on the previous findings, a reduced rate of xylose or other sugar consumption by *E.*
479 *coli* monoculture at the initial stages might lead to a decreased ethanol yield. Because the specific
480 productivity of ethanol is maximum during the log phase to the early stationary phase while *E. coli*
481 mainly consumes xylose after exhaustion of glucose or reaching this sugar at a certain level (Wang
482 et al., 2019). Another ethanologenic microorganism is *S. cerevisiae*, which is widely applied in
483 ethanol fermentation due to its exceptional capacity to ferment hexose sugars such as glucose and
484 fructose, along with sucrose (Qiu et al., 2023). Despite these capabilities, the inability to ferment
485 pentose sugars by natural strains of this yeast is a notable limitation (Ochoa-Chacón et al., 2022).
486 In this context, the use of a coculture system was assumed to be more promising to further improve
487 ethanol yield. Considering the compatibility, the coculture of *S. cerevisiae* and *Scheffersomyces*
488 *stipitis* would be a superior option for ethanol production from mixed sugars. This preference arises
489 from the fact that both species serve as complementary metabolizers of pentose (*S. stipites*) and
490 hexose (*S. cerevisiae*) sugars. Nevertheless, pentose metabolism by *S. stipitis* in the presence of *S.*
491 *cerevisiae* is problematic as the former needs fixed specific oxygen (qO_2) for pentose metabolism,
492 where *S. cerevisiae* interferes (Chen, 2011). Consequently, to address the slower xylose and
493 fructose consumption observed in co-fermentation with *E. coli* monoculture (Section 3.1), an *E.*
494 *coli-S. cerevisiae* coculture system was employed. The rationale behind this choice was the

495 anticipation that such a system could facilitate the rapid consumption of glucose in the initial
496 stages. This, in turn, would expedite the attainment of the critical level of glucose, thereby enabling
497 the subsequent consumption of other sugars, including xylose. Moreover, the use of coculture
498 systems is an emerging technology, which has recently attracted significant attraction in ethanol
499 and chemicals production (Akdemir et al., 2022).

500
501 To exploit *E. coli*-yeast coculture, several concerns should be appropriately addressed, with
502 particular emphasis on selecting suitable medium compositions for both strains. As discussed in
503 the method section, seed cultures of *E. coli* and *S. cerevisiae* were performed in LB broth and YPD
504 broth, respectively. At this stage, co-fermentation was conducted in a modified LB medium for
505 both strains, which was prepared by enriching the hydrolysate with components of the LB medium.
506 A similar medium composition was also used to grow both *E. coli* and *S. cerevisiae* in a coculture
507 system without any significant interference in the growth (Li et al., 2010). We also found over
508 99% growth of *E. coli* and 94% growth of *S. cerevisiae*, in comparison to their growth in the
509 respective medium (Fig. 3a). To determine the most favorable conditions for both strains within
510 the coculture system, the growth of both strains was assessed under varying pH (5, 6, and 7) and
511 temperature levels (30, 33, 35, and 37 °C) using a ratio of 1:1 of both strains and LB medium
512 supplemented with 50 g/L glucose and 20 g/L xylose. Growth was evaluated by measuring the
513 OD₆₀₀ after 24 h. The results were compared with the growth of the individual strains in the same
514 medium under their respective optimum conditions (pH 7.0 and 37 °C for *E. coli*; pH 5.0 and 30
515 °C for yeast). The findings indicated that more than 90% of the growth of both strains was achieved
516 at pH 6.0 and temperature 35 °C (Fig. 3b). Almost similar conditions (pH 6.4 and 37 °C) were also
517 used in a previous study for *E. coli*-yeast coculture used to produce ethanol from biomass slurries
518 (Wang et al., 2019).

519

520 **Fig. 3**

521

522 3.2.2. SHCF of WS slurries by *E. coli*-yeast coculture

523 The *E. coli*-yeast coculture was used in the SHCF of hydrolysate using a ratio (*E. coli*: *S.*
524 *cerevisiae*) of 3:1. Following a preliminary trial, the *E. coli* concentration was maintained at three
525 times that of the yeast, taking into account the longer time required for xylose fermentation by *E.*

526 *coli*. The total initial inoculum size was around 4×10^6 CFU/ml (equivalent to 6.6 log₁₀ CFU/ml).
527 As depicted in Fig. 3c, the growth pattern of *E. coli* closely mirrored that observed in its
528 monoculture (Fig. 2a). The average bacterial cell count varied from 6.62 log₁₀ CFU/ml after 6 h
529 to 6.77 log₁₀ CFU/ml after 24 h, which continued to slightly increase until 72 h and peaked at 6.79
530 log₁₀ CFU/ml, and then gradually declined. The yeast cells grow exponentially until 18 h with the
531 cell count reaching 6.55 log₁₀ CFU/ml (Fig. 3c). Thereafter, a slight increase in yeast cell growth
532 was observed, reaching 6.59 log₁₀ CFU/ml after 96 h and was almost the same at the end of
533 fermentation (120 h). These findings suggest that yeast demonstrated greater tolerance during co-
534 fermentation than *E. coli* cells, which is supported by literature indicating high tolerance of yeast
535 to ethanol and inhibitors (Pereira et al., 2016). Therefore, the observed low tolerance of *E. coli*
536 cells during both monoculture and coculture fermentations might be attributable to the cumulative
537 stress arising from inhibitors, sugars, and ethanol.

538

539 In comparison to the monoculture system, the coculture system demonstrated a notably
540 accelerated rate of ethanol production up to 24 h ($P < 0.01$). As a result, ethanol titer reached 25.47
541 g/L after 24 h (Fig. 3d), marking a 56% increase over the titer achieved by *E. coli* monoculture.
542 This, in turn, resulted in higher volumetric ethanol productivity, 1.06 g/L/h after 24 h, than
543 monoculture technology (Fig. 3d). These findings were consistent with those reported in an earlier
544 study, which highlighted a significant increase in both ethanol titer and productivity, up to 26%
545 and 29%, respectively, compared to the monoculture (Unrean and Khajeeram, 2015). The elevated
546 titer and productivity of ethanol were attributed to the accelerated consumption of sugars, notably
547 glucose, by both *E. coli* and *S. cerevisiae* at the initial stages of fermentation. This assertion is
548 supported by the considerable reduction in available glucose to 14.23 g/L after 24 h (Fig. 3e). In
549 addition, there was a considerable decrease in fructose concentration to 6.41 g/L during this period
550 (Fig. 3e).

551

552 As a result, ethanol titer increased to 38.73 g/L after 48 h (Fig 3d), which continued to rise
553 until 96 h, reaching 48.61 g/L after 96 h. However, there was no significant increase in ethanol
554 titer thereafter ($P > 0.05$), which could be attributed to the incomplete consumption of xylose as *E.*
555 *coli* cells entered a decline phase, alongside a halt in the metabolism of glucose and fructose.
556 Consequently, a notable amount of xylose (21.23 g/L) and considerable amounts of glucose (7.26

557 g/L) and fructose (4.62 g/L) remained unconverted after fermentation (Fig. 3e). The pattern of
558 sugar consumption observed in this study aligned closely with a prior study (Lau et al., 2010),
559 which reported a faster glucose consumption rate by *S. cerevisiae* as it consumed 100 g/L in 24 h
560 while *E. coli* took 72 h to consume the same amount of glucose. Conversely, the consumption of
561 sugars in the presence of xylose was markedly slower, to the extent that even after 168 h, 100 g/L
562 of total xylose and glucose could not be fully consumed, with the majority of sugar consumption
563 occurring within the initial 48 h (Lau et al., 2010). The theoretical ethanol yield also rose
564 significantly to nearly 67% at the end of fermentation (Fig. 3d). Nonetheless, despite this
565 significant enhancement in ethanol yield brought about by the coculture technology, this yield was
566 still relatively lower. This low yield was not only due to the decreased consumption of available
567 sugars, particularly xylose but also the production of byproducts. In contrast to the byproduct
568 generation by *E. coli* monoculture, co-fermentation of hydrolysate using coculture technology
569 exhibited a significant amount of glycerol as a byproduct, with the final concentration reaching
570 approximately 5.5 g/L (Fig. 3f). The elevated accumulation of glycerol under the coculture system
571 was attributed to the metabolic activities of the yeast cells as the sole contributor, which was also
572 reported earlier during the co-fermentation of xylose and glucose (Lau et al., 2010). In fact, *S.*
573 *cerevisiae* possesses an efficient metabolic pathway to convert sugars into glycerol, while *E. coli*
574 is usually devoid of such metabolic pathways. In particular, sugars can be converted into glycerol
575 in *S. cerevisiae* by the action of two crucial enzymes, namely glycerol-3-phosphate dehydrogenase
576 (GPD1) and glycerol-3-phosphatase (GPP2), as reported earlier (Heo et al., 2019). Due to the
577 absence of these two enzymes in *E. coli*, it contributed virtually no glycerol during co-
578 fermentation. In addition to glycerol, there was either a minor or significant upsurge in other
579 byproducts, including formate, acetate, and lactate (Fig. 3f).

580

581 3.3. Effects of additives and inhibitors on co-fermentation of hydrolysate

582

583 Based on the overall findings discussed above, it is reasonable to infer that enhancing xylose
584 consumption is important to further improve ethanol yield and titer. Nevertheless, the consumption
585 of xylose by *E. coli*, whether in monoculture or coculture, requires a longer duration compared to
586 that of glucose or fructose (Akter et al., 2020). On the other hand, bacterial cells experienced a
587 shorter stationary phase, transitioning into a decline phase after 96 h, irrespective of their presence

588 in monoculture or coculture (Fig. 2a and 3c). Moreover, despite a notable enhancement in the
589 consumption of glucose and fructose achieved by incorporating yeast in the microbial systems, the
590 consumption of both sugars was slow either during the later stages (glucose) or the initial stages
591 (fructose and xylose), thus preventing complete utilization of these sugars. It was assumed that
592 two primary issues could underlie these constraints. First, to counter the impacts of inhibitory
593 components on the enzymatic cellulose hydrolysis, the slurries were supplemented with additives
594 such as syringic acid and polyethylene glycol during pretreatment and hydrolysis, respectively.
595 Therefore, it is important to evaluate if there were any impacts of these additives on cells.
596 Secondly, growth inhibition might have also resulted from inhibitors present in the hydrolysates.
597 Hence, further experiments were conducted to evaluate and address these issues, and the results
598 are illustrated in Fig.4.

599

600 To investigate the impacts of syringic acid addition during pretreatment and polyethylene
601 glycol during hydrolysis, a modified hydrolysate was produced by avoiding such supplementation.
602 One set of this hydrolysate was then detoxified to assess the effects of inhibitors on ethanol
603 fermentation. Given that the sugar concentration in these hydrolysates was lower than that of the
604 hydrolysates obtained from the optimal configuration (data not shown), sugar concentrations were
605 adjusted to match the composition of the main hydrolysate. This adjustment was made by
606 incorporating respective sugars from an external source. Co-fermentation was then carried out
607 using a coculture system under the optimal configuration. Results showed that there were
608 significant variations ($P>0.05$) in growth and ethanol yield between experiments with and without
609 supplementing additives, particularly when the hydrolysate was not detoxified before fermentation
610 (Fig. 4a,d). Notably, the growth of *E. coli* appeared to be more severely impacted compared to that
611 of yeast cells. The *E. coli* cell count dropped to 6.72 log₁₀ CFU/ml after 72 h, while the yeast
612 count decreased to 6.56 log₁₀ CFU/ml during the same period (Fig. 4a). As a consequence, the
613 final ethanol yield decreased to 58.43%, while the levels of residual sugars escalated to 54.27 g/L
614 (Fig. 4d). These findings suggest that the presence of additives in the hydrolysate did not affect
615 microbial growth and ethanol yield. Instead, it significantly influenced both the efficiency of
616 growth and fermentation. Previous studies have also suggested that additives, especially
617 polyethylene glycol or other surfactants, can augment microbial growth and fermentation by
618 enhancing microbial interaction and buffering capacity (Singh et al., 2021).

619

620 Detoxification of hydrolysate before fermentation led to significant improvements in both
621 cell count and ethanol yield (Fig. 4b,e), compared to the undetoxified conditions (without
622 additives). Interestingly, cell count and ethanol yield were even higher after detoxification than
623 those obtained from the SHCF with the addition of syringic acid and polyethylene glycol under
624 undetoxified conditions. After detoxification, the final ethanol yield increased to 74.95% (Fig. 4e),
625 while the growth of *E. coli* and yeast increased to 6.81 log₁₀ CFU/ml and 6.62 log₁₀ CFU/ml,
626 respectively after 96 h (Fig. 4b). Accordingly, the concentration of residual sugars dropped to
627 33.05 g/L (Fig. 4e), primarily due to the enhanced consumption of glucose and fructose. However,
628 the consumption of xylose did not exhibit any significant changes even after detoxification. These
629 findings imply that there might be an effect of inhibitors on fermentation, despite the strains being
630 previously evolved. It is not surprising that the strains may exhibit reduced tolerance to inhibitors
631 in a new environment, even if they were previously adapted to specific conditions, as the overall
632 conditions can vary depending on the biomass and processing parameters. Moreover, the lower
633 tolerance of the evolved strains might also be attributed to the combined stress arising from both
634 inhibitors and fermentation metabolites like ethanol, as discussed earlier for *E. coli* (Jin et al.,
635 2012).

636

637 Although a prior detoxification could improve ethanol yield, a separate detoxification step
638 might introduce technical complications. Therefore, to address the effects of inhibitors
639 alternatively, the undetoxified hydrolysate (with syringic acid and polyethylene glycol treatments)
640 was supplemented with 1.0 mM of betaine and 2.6 mM of sodium metabisulfite before
641 fermentation to reduce the toxicity of the undetoxified hydrolysate, as discussed before (Wang et
642 al., 2019). The purpose of this supplementation was to attain an ethanol yield comparable to that
643 achieved from the detoxified hydrolysate, thereby avoiding the need for a separate detoxification
644 step. It was found that microbial growth was significantly higher than the respective undetoxified
645 hydrolysate (Fig. 4c). Moreover, there was an insignificant ($P>0.05$) variation in microbial growth
646 between detoxified and undetoxified (but supplemented with betaine and Na- metabisulfite)
647 hydrolysates. As shown in Fig. 4f, ethanol titer increased to 53.18 g/L, with the yield reaching
648 ~73%, after supplementing the undetoxified hydrolysate with betaine and Na- metabisulfite. This
649 represented a 25% increase compared to that obtained from the undetoxified hydrolysate without

650 such a supplementation. Nevertheless, the final ethanol yield (73%) under this supplementation
651 condition remained below that reported in some earlier studies. For example, the maximum ethanol
652 yield was reported at 87.5% (Jung et al., 2013). This lower yield could be attributed to the effects
653 of soluble sugars, with notably higher levels of total sugars present in the hydrolysate of HSS
654 (Table 1). These high sugar levels might constrain the consumption of xylose during fermentation
655 since xylose nearly remained unconverted after fermentation.

656

657 **Fig. 4**

658

659 3.4. DP-SSCF

660

661 It was assumed that high sugar concentrations in hydrolysate increased the stress conditions
662 for microorganisms during SHCF, affecting both sugar consumption and ethanol yield by exerting
663 additional stress on the cells. Therefore, a further configuration was done in co-fermentation
664 technology by exploring DP-SSCF, in which pretreated slurry obtained from pretreatment was
665 directly used in the co-fermentation without prior cellulose hydrolysis. The composition of
666 pretreated slurry is presented in Table 1. In this configuration, the sugars found in the pretreated
667 slurry were initially allowed to be consumed by microorganisms in the first phase, while the second
668 phase was designed for concurrent cellulose hydrolysis and consumption of the resulting glucose.
669 The DP-SSCF was configured in two different ways: (1) using *E. coli* and yeast in separate phases,
670 designated as the first and second phases, respectively (hereafter, DP-SSCF-E/S). The optimum
671 pH (7.0 for *E. coli* and 5.0 for yeast) and temperature (37 °C for *E. coli* and 30 °C for yeast) were
672 maintained for each strain. (2) A coculture was used in the first phase to promote the consumption
673 of initial sugars, with yeast employed in the second phase to effectively utilize glucose derived
674 from cellulose (hereafter, DP-SSCF-ES/S). In this setup, the pH and temperature of the first phase
675 were the same as used for the coculture (pH 6 and temperature 35 °C), while the optimum
676 conditions for the yeast were maintained in the second phase (pH 5 and temperature 30 °C). In
677 both cases, total inoculum and nutrients were kept the same.

678

679 The use of coculture was found to expedite sugar consumption during both the first and
680 second phases, leading to the nearly complete depletion of sugars present in the pretreated slurry

681 within 48 h. In contrast, *E. coli* monoculture in DP-SSCF-E/S required 72 h to consume the sugars
682 of the pretreated slurry. Therefore, the second phase was initiated after 60 h in DP-SSCF-E/S and
683 36 h in DP-SSCF-ES/S to avoid the lag phase in ethanol production. It was found that a small
684 portion of the total released sugars remained unconverted at the end of DP-SSCF, which were 6.58
685 g/L in DP-SSCF-E/S and 4.15 g/L in DP-SSCF-ES/S (Fig. 5a). This small variation in total
686 residual sugars between the two approaches was mainly due to the glucose (Fig. 5b) as the other
687 two major sugars (xylose and fructose) were very close in DP-SSCF-E/S and DP-SSCF-ES/S (Fig.
688 5c,d). This might be because the second phase in both techniques was started when initial sugars
689 (present in the pretreated slurry) reached critical levels, despite the different durations, while
690 hydrolysis of a small amount of (residual) hemicellulose present in the pretreated slurry occurred
691 similarly in each approach. This was supported by the close hydrolysis yield of residual
692 hemicellulose in the two DP-SSCF technologies (93.05% vs. 93.33%), as illustrated in Fig. 5e. On
693 the other hand, cellulose hydrolysis yield was lower in DP-SSCF-E/S compared to that achieved
694 from DP-SSCF-ES/S, amounting to 95.58% and 97.91%, respectively (Fig. 5e). An excellent
695 cellulose hydrolysis yield under DP-SSCF might be due to the presence of lower sugars during
696 cellulose hydrolysis in the second phase, favoring the hydrolysis process. Accordingly, a negligible
697 amount of hemicellulose and a small portion of cellulose remained as residual at the end of DP-
698 SSCF (Fig. 5f). In both methods, the lignin content after DP-SSCF did not differ significantly from
699 that present in the pretreated slurry (Fig. 5f, Table 1). This is because neither the conditions of DP-
700 SSCF were conducive enough to induce changes in lignin nor could the microorganisms utilize
701 lignin. In summary, all types of sugars, including xylose, exhibited more efficient consumption
702 under DP-SSCF compared to that occurred in SHCF, with DP-SSCF-ES/S demonstrating superior
703 efficiency and a shorter sugar consumption time.

704

705 **Fig. 5**

706

707 Corresponding to the sugar consumption pattern, DP-SSCF-E/S needed 120 h to attain the
708 peak ethanol titer of 59.6 g/L, while DP-SSCF-ES/S exhibited a peak ethanol titer of 63.14 g/L
709 within 72 h (Fig. 6a), owing to the accelerated sugar consumption (except xylose) by yeast in both
710 first and second phases. The comparatively sluggish rate of ethanol production by *E. coli*
711 monoculture primarily resulted from the slower consumption of xylose in the presence of glucose

712 (Dev et al., 2022). Accordingly, both the yield and productivity of ethanol exhibited variation
713 between the two configurations (Fig. 6c,d). The highest recorded ethanol yield was 84.3% with
714 DP-SSCF-ES/S, while with DP-SSCF-E/S, it stood at 79.6% (Fig. 6b). Exhibiting a gradual
715 decline, the final ethanol productivity, as determined at the peak of ethanol production, was
716 recorded at 0.88 g/L/h after 72 h with DP-SSCF-ES/S and 0.5 g/L/h after 120 h with DP-SSCF-
717 E/S (Fig. 6c). In summary, compared to SHCF technology, the ethanol titer in DP-SSCF was
718 significantly higher, with 12.2% in DP-SSCF-E/S and 19.56% in DP-SSCF-ES/S. Thus, the DP-
719 SSCF-ES/S configuration was considered the optimal choice for ethanol production from HSS,
720 considering its maximum ethanol yield, titer, and productivity.

721

722 **Fig. 6**

723

724 The byproduct formation pattern closely resembled that of the SHCF under the coculture
725 system, except for glycerol, which exhibited higher levels in the later stages of DP-SSCF,
726 corresponding to the yeast addition time (Fig. 5c,d). Glycerol remained the dominant byproduct,
727 ranging from 5.14 to 5.73 g/L. The final quantities of lactate, formate, and acetate did not
728 significantly differ between DP-SSCF-E/S, DP-SSCF-ES/S, and SHCF. The superior ethanol yield
729 achieved with DP-SSCF in comparison to SHCF, under identical conditions (*i.e.*, without
730 detoxification), suggests that the growth and metabolic functions of microorganisms, especially *E.*
731 *coli*, were influenced not only by the presence of inhibitors but also by elevated concentrations of
732 sugars, ethanol, and other fermentation byproducts.

733

734 The ethanol titer achieved in this study through the DP-SSCF-ES/S strategy was notably
735 higher than that reported for ethanol production from lignocellulosic biomass. Previous studies
736 have shown varying yields, ranging from 12.1 g/L using *Miscanthus giganteus* (Scordia et al.,
737 2013) to 55.5 g/L using reed (Li et al., 2009), with a productivity of 0.13 g/L/h and 0.57 g/L/h,
738 respectively. In contrast, this study recorded an impressive ethanol titer of 63.14 g/L, with a
739 productivity of 0.88 g/L/h. On the other hand, a higher ethanol titer was reported using *M.*
740 *sacchariflorus*, reaching 69.2 g/L titer with 1.24 g/L/h productivity and 87.2% yield. However, it
741 employed a continuous feeding approach and a specialized reactor with an angled-type impeller,
742 contributing to the achievement of the high ethanol yield. In comparison, this study was conducted

743 through the flask fermentation approach. Similarly, a recent study reported a higher productivity
744 of 1.86 g/L/h by employing the combined utilization of solid and liquid fractions of pretreated
745 sugarcane bagasse (Perez et al., 2023). The authors used a recombinant yeast in their study,
746 suggesting that additional metabolic modifications to the strains used in the present work could
747 further augment ethanol production from sugary stovers. In another study, an integrated approach
748 involving a blend of corn stover (10%) and corn grains (20%) yielded up to 104.9 g/L of ethanol
749 (Chen et al., 2018). However, it is important to consider the ongoing debate regarding the use of
750 corn grains for food versus fuel, as the ethanol fermentability of starchy grains like corn is notably
751 higher than that of lignocellulosic biomass (Zabed et al., 2017). In contrast, considering the
752 promising role of soluble sugars in lignocellulosic ethanol production as identified in this study,
753 future attempts could be made to integrate sugary wastes (e.g. molasses) with other biomass. In
754 this context, further process optimization at scale-up studies should be given research priority.

755

756 **4. Conclusion**

757

758 The study assessed microbial systems and process configurations for ethanol production from
759 HSS. The co-fermentation of undetoxified hydrolysate with *E. coli* monoculture and *E. coli*-*S.*
760 *cerevisiae* coculture revealed that there is an effect of inhibitors and soluble sugars on ethanol
761 yield and titer. Further, the metabolism of xylose and fructose in the presence of glucose also
762 resulted in a lower ethanol yield. To resolve these issues, a double phase-SSCF strategy was
763 explored to introduce cellulose-derived glucose after consumption of sugars (particularly, xylose
764 and fructose) present in the pretreated slurry. Further, the impact of inhibitors was alleviated by
765 incorporating betaine and sodium metabisulfite into the hydrolysate. These modifications resulted
766 in enhanced ethanol production, with a titer of 63.14 g/L, yield of 84.3%, and productivity of 0.88
767 g/L/h. Despite the promising findings in this study, the use of double phase-SSCF with the required
768 supplementation of chemicals and enzymes may raise some concerns. Therefore, there is a need
769 for further research to explore alternative strategies, leveraging recent developments in synthetic
770 biology, to reduce or minimize inputs and process steps. For example, stable enzyme systems could
771 be developed by exploring multienzyme cascades on advanced materials like macromolecular
772 scaffolds or nanomaterials, which could eliminate the necessity of adding a carbocation agent.
773 Additionally, on-site expression of necessary enzymes through surface display technology could

774 eliminate the reliance on external enzymes. Likewise, the use of co-culture could be avoided by
775 developing cell factories through rational engineering in a single strain. This could involve
776 enhancing xylose and fructose metabolism by addressing glucose preference issues, incorporating
777 absent pathways (e.g., xylose metabolism pathway in yeast), or overexpressing sluggish pathways
778 (e.g., xylose metabolism pathway in *E. coli*). Furthermore, the need for betaine and sodium
779 metabisulfite, used to reduce the toxicity of inhibitors, could be obviated by developing high-
780 tolerant strains through rational or omics-mediated metabolic engineering, genome minimization
781 technology, or global transcription machinery engineering. With successful developments through
782 these efforts and subsequent scale-up studies, it is anticipated that a sustainable technology for
783 large-scale ethanol production from sugary stovers can be achieved.

784

785 **Acknowledgements**

786

787 We are grateful to the Key R&D Program (Grant No. 2022YFC2105501).

788

789 **References**

790 Aggarwal, N.K., Kumar, N., Mittal, M., 2022. Ethanogenic Bacteria: Present Status for Bioethanol
791 Production, in: He, L., Tundo, P.Z., Zhang, C. (Eds), Green Chemistry and Sustainable
792 Technology. Springer International Publishing, Cham, pp. 137-147.

793 Akdemir, H., Liu, Y., Zhuang, L., Zhang, H., Koffas, M.A.G., 2022. Utilization of
794 microbial cocultures for converting mixed substrates to valuable bioproducts. *Curr. Opin.*
795 *Microbiol.* 68, 102157. <http://dx.doi.org/10.1016/j.mib.2022.102157>.

796 Akter, S., Zayed, H.M., Sahu, J.N., Chowdhury, F.I., Faruq, G., Boyce, A.N., Qi, X.H., 2020.
797 Bioethanol production from water-soluble and structural carbohydrates of normal and high
798 sugary corn stovers harvested at three growth stages. *Energy Convers. Manage.* 221, 113104.
799 <http://dx.doi.org/10.1016/j.enconman.2020.113104>.

800 Barros-Rios, J., Romani, A., Garrote, G., Ordas, B., 2015. Biomass, sugar, and bioethanol potential
801 of sweet corn. *GCB Bioenergy* 7, 153-160. <http://dx.doi.org/10.1111/gcbb.12136>.

802 Bozell, J.J., Petersen, G.R., 2010. Technology development for the production of biobased
803 products from biorefinery carbohydrates—the US Department of Energy’s “Top 10” revisited.
804 Green Chem. 12, 539-554. <http://dx.doi.org/10.1039/B922014C>.

805 Bukhari, N.A., Loh, S.K., Luthfi, A.A.I., Abdul, P.M., Nasrin, A.B., Harun, S., Jahim, J.M., 2021.
806 Whole slurry saccharification of mild oxalic acid-pretreated oil palm trunk biomass improves
807 succinic acid production. Ind. Crop Prod. 171, 113854.
808 <http://dx.doi.org/10.1016/j.indcrop.2021.113854>.

809 Chen, S., Xu, Z., Li, X., Yu, J., Cai, M., Jin, M., 2018. Integrated bioethanol production from
810 mixtures of corn and corn stover. Bioresour. Technol. 258, 18-25.
811 <http://dx.doi.org/10.1016/j.biortech.2018.02.125>.

812 Chen, Y., 2011. Development and application of co-culture for ethanol production by co-
813 fermentation of glucose and xylose: a systematic review. J. Ind. Microbiol. Biotechnol. 38, 581-
814 597. <https://doi.org/10.1007/s10295-010-0894-3>

815 da Silva, A.S.A., Espinheira, R.P., Teixeira, R.S.S., de Souza, M.F., Ferreira-Leitão, V., Bon, E.P.,
816 2020. Constraints and advances in high-solids enzymatic hydrolysis of lignocellulosic biomass:
817 a critical review. Biotechnol. Biofuel 13, 58. <http://dx.doi.org/10.1186/s13068-020-01697-w>.

818 del Río, P.G., Gullón, P., Rebelo, F., Romaní, A., Garrote, G., Gullón, B., 2020. A whole-slurry
819 fermentation approach to high-solid loading for bioethanol production from corn stover.
820 Agronomy 10, 1790. <http://dx.doi.org/10.3390/agronomy10111790>.

821 Dev, C., Jilani, S.B., Yazdani, S.S., 2022. Adaptation on xylose improves glucose–xylose co-
822 utilization and ethanol production in a carbon catabolite repression (CCR) compromised
823 ethanologenic strain. Microb. Cell Fact. 21, 154. [http://dx.doi.org/10.1186/s12934-022-01879-](http://dx.doi.org/10.1186/s12934-022-01879-1)
824 [1](http://dx.doi.org/10.1186/s12934-022-01879-1).

825 Fernández-Sandoval, M.T., Galíndez-Mayer, J., Bolívar, F., Gosset, G., Ramírez, O.T., Martínez,
826 A., 2019. Xylose–glucose co-fermentation to ethanol by Escherichia coli strain MS04 using
827 single- and two-stage continuous cultures under micro-aerated conditions. Microb. Cell Fact.
828 18, 145. <http://dx.doi.org/10.1186/s12934-019-1191-0>.

829 Gao, Y., Xu, J., Yuan, Z., Zhang, Y., Liu, Y., Liang, C., 2014. Optimization of fed-batch enzymatic
830 hydrolysis from alkali-pretreated sugarcane bagasse for high-concentration sugar production.
831 Bioresour. Technol. 167, 41-45. <http://dx.doi.org/10.1016/j.biortech.2014.05.034>.

832 He, D., Chen, X., Lu, M., Shi, S., Cao, L., Yu, H., Lin, H., Jia, X., Han, L., Xiao, W., 2023. High-
833 solids saccharification and fermentation of ball-milled corn stover enabling high titer bioethanol
834 production. Renew. Energy 202, 336-346. <http://dx.doi.org/10.1016/j.renene.2022.11.096>.

835 Heo, W., Kim, J.H., Kim, S., Kim, K.H., Kim, H.J., Seo, J.H., 2019. Enhanced production of 3-
836 hydroxypropionic acid from glucose and xylose by alleviation of metabolic congestion due to
837 glycerol flux in engineered *Escherichia coli*. Bioresour. Technol. 285, 121320.
838 <https://doi.org/10.1016/j.biortech.2019.121320>.

839 Hilares, R.T., Muñoz, S.S., Alba, E.M., Prado, C.A., Ramos, L., Ahmed, M.A., da Silva, S.S.,
840 Santos, J.C., 2022. Recent technical advancements in first, second and third generation ethanol
841 production, in: Chandel, A.K., Segato, F., Production of Top 12 Biochemicals Selected by
842 USDOE from Renewable Resources. Elsevier Inc., pp. 203-232.

843 Jarunglumlert, T., Prommuak, C., 2021. Net energy analysis and techno-economic assessment of
844 co-production of bioethanol and biogas from cellulosic biomass. Fermentation 7, 229.
845 <http://dx.doi.org/10.3390/fermentation7040229>.

846 Jin, M., Balan, V., Gunawan, C., Dale, B.E., 2012. Quantitatively understanding reduced xylose
847 fermentation performance in AFEXTM treated corn stover hydrolysate using *Saccharomyces*
848 *cerevisiae* 424A (LNH-ST) and *Escherichia coli* KO11. Bioresour. Technol. 111, 294-300.
849 <http://dx.doi.org/10.1016/j.biortech.2012.01.154>.

850 Jung, Y.H., Kim, I.J., Kim, H.K., Kim, K.H., 2013. Dilute acid pretreatment of lignocellulose for
851 whole slurry ethanol fermentation. Bioresour. Technol. 132, 109-114.
852 <http://dx.doi.org/https://doi.org/10.1016/j.biortech.2012.12.151>.

853 Kim, J.K., Yang, J., Park, S.Y., Yu, J.-H., Kim, K.H., 2019. Cellulase recycling in high-solids
854 enzymatic hydrolysis of pretreated empty fruit bunches. Biotechnol. Biofuel 12, 138.
855 <http://dx.doi.org/10.1186/s13068-019-1476-x>.

856 Ko, Y.-S., Kim, J.W., Lee, J.A., Han, T., Kim, G.B., Park, J.E., Lee, S.Y., 2020. Tools and
857 strategies of systems metabolic engineering for the development of microbial cell factories for
858 chemical production. *Chem. Soc. Rev.* 49, 4615-4636. <https://doi.org/10.1039/D0CS00155D>.

859 Lau, M.W., Gunawan, C., Balan, V., Dale, B.E., 2010. Comparing the fermentation performance
860 of *Escherichia coli* KO11, *Saccharomyces cerevisiae* 424A(LNH-ST) and *Zymomonas mobilis*
861 AX101 for cellulosic ethanol production. *Biotechnol. Biofuel* 3, 11-11.
862 <http://dx.doi.org/10.1186/1754-6834-3-11>.

863 Lewandrowski, J., Rosenfeld, J., Pape, D., Hendrickson, T., Jaglo, K., Moffroid, K., 2020. The
864 greenhouse gas benefits of corn ethanol – assessing recent evidence. *Biofuels* 11, 361-375.
865 <http://dx.doi.org/10.1080/17597269.2018.1546488>.

866 Li, H., Kim, N.-J., Jiang, M., Kang, J.W., Chang, H.N., 2009. Simultaneous saccharification and
867 fermentation of lignocellulosic residues pretreated with phosphoric acid–acetone for bioethanol
868 production. *Bioresour. Technol.* 100, 3245-3251.
869 <http://dx.doi.org/10.1016/j.biortech.2009.01.021>.

870 Li, J., Xu, Y., Zhang, M., Wang, D., 2017. Determination of furfural and 5-hydroxymethylfurfural
871 in biomass hydrolysate by high-performance liquid chromatography. *Energy Fuel* 31, 13769-
872 13774. <https://doi.org/10.1021/acs.energyfuels.7b02827>.

873 Li, X., Kim, T.H., Nghiem, N.P., 2010. Bioethanol production from corn stover using aqueous
874 ammonia pretreatment and two-phase simultaneous saccharification and fermentation (TPSSF).
875 *Bioresour. Technol.* 101, 5910-5916. <http://dx.doi.org/10.1016/j.biortech.2010.03.015>.

876 Liu, L., Zhang, Z., Wang, J., Fan, Y., Shi, W., Liu, X., Shun, Q., 2019. Simultaneous
877 saccharification and co-fermentation of corn stover pretreated by H₂O₂ oxidative degradation
878 for ethanol production. *Energy* 168, 946-952. <https://doi.org/10.1016/j.energy.2018.11.132>.

879 Malik, K., Sharma, P., Yang, Y., Zhang, P., Zhang, L., Xing, X., Yue, J., Song, Z., Nan, L., Yujun,
880 S., El-Dalatony, M.M., Salama, E.-S., Li, X., 2022. Lignocellulosic biomass for bioethanol:
881 Insight into the advanced pretreatment and fermentation approaches. *Ind. Crop Prod.* 188,
882 115569. <http://dx.doi.org/10.1016/j.indcrop.2022.115569>.

883 Moxley, G., Gaspar, A.R., Higgins, D., Xu, H., 2012. Structural changes of corn stover lignin
884 during acid pretreatment. *J. Ind. Microbiol. Biotechnol.* 39, 1289-1299.
885 <http://dx.doi.org/10.1007/s10295-012-1131-z>.

886 Müller, L., Gnoyke, S., Popken, A.M., Böhm, V., 2010. Antioxidant capacity and related
887 parameters of different fruit formulations. *LWT-Food Sci. Technol.* 43, 992-999.
888 <http://dx.doi.org/10.1016/j.lwt.2010.02.004>.

889 Noppawan, P., Lanctot, A.G., Magro, M., Navarro, P.G., Supanchaiyamat, N., Attard, T.M., Hunt,
890 A.J., 2021. High pressure systems as sustainable extraction and pre-treatment technologies for
891 a holistic corn stover biorefinery. *BMC Chem.* 15, 37. [http://dx.doi.org/10.1186/s13065-021-](http://dx.doi.org/10.1186/s13065-021-00762-1)
892 [00762-1](http://dx.doi.org/10.1186/s13065-021-00762-1).

893 Ntakirutimana, S., Xu, T., Ding, M.-Z., Liu, Z.-H., Li, B.-Z., Yuan, Y.-J., 2023. Chemomechanical
894 pretreatment for efficient delignification and saccharification of corn stover biomass. *Chem.*
895 *Eng. J.* 471, 144588. <http://dx.doi.org/10.1016/j.cej.2023.144588>.

896 Ochoa-Chacón, A., Martinez, A., Poggi-Varaldo, H.M., Villa-Tanaca, L., Ramos-Valdivia, A.C.,
897 Ponce-Noyola, T., 2022. Xylose metabolism in bioethanol production: *Saccharomyces*
898 *cerevisiae* vs non-*Saccharomyces* yeasts. *BioEnergy Res.* 15, 905-923.
899 <http://dx.doi.org/10.1007/s12155-021-10340-x>.

900 Peng, J., Xu, Y., Zhu, B., Yu, H., Li, B., Xu, H., 2023. Life cycle assessment of bioethanol
901 production by two methods of pretreatment of rice straw based on process simulation. *Ind. Crop*
902 *Prod.* 191, 115810. <http://dx.doi.org/10.1016/j.indcrop.2022.115810>.

903 Pereira, J.P.C., Verheijen, P.J.T., Straathof, A.J.J., 2016. Growth inhibition of *S. cerevisiae*, *B.*
904 *subtilis*, and *E. coli* by lignocellulosic and fermentation products. *Appl. Microbiol. Biotechnol.*
905 100, 9069-9080. <http://dx.doi.org/10.1007/s00253-016-7642-1>.

906 Perez, C.L., Milessi, T.S., Sandri, J.P., Ramos, M.D., Carvalho, B.T., Claes, A., Demeke, M.M.,
907 Thevelein, J.M., Zangirolami, T.C., 2023. Evaluation of consolidated bioprocessing of
908 sugarcane biomass by a multiple hydrolytic enzyme producer *Saccharomyces* yeast. *BioEnergy*
909 *Res.* 16, 1973–1989. <https://doi.org/10.1007/s12155-023-10607-5>

910 Periyasamy, S., Beula Isabel, J., Kavitha, S., Karthik, V., Mohamed, B.A., Gizaw, D.G.,
911 Sivashanmugam, P., Aminabhavi, T.M., 2023. Recent advances in consolidated bioprocessing
912 for conversion of lignocellulosic biomass into bioethanol – A review. Chem. Eng. J. 453,
913 139783. <http://dx.doi.org/10.1016/j.cej.2022.139783>.

914 Qin, L., Li, X., Liu, L., Zhu, J.-Q., Guan, Q.-M., Zhang, M.-T., Li, W.-C., Li, B.-Z., Yuan, Y.-J.,
915 2017. Dual effect of soluble materials in pretreated lignocellulose on simultaneous
916 saccharification and co-fermentation process for the bioethanol production. Bioresour. Technol.
917 224, 342-348. <http://dx.doi.org/10.1016/j.biortech.2016.11.106>.

918 Qiu, Y., Wu, M., Bao, H., Liu, W., Shen, Y., 2023. Engineering of *Saccharomyces cerevisiae* for
919 co-fermentation of glucose and xylose: current state and perspectives. Eng. Microbiology, 3,
920 100084. <http://dx.doi.org/10.1016/j.engmic.2023.100084>.

921 Rathour, R.K., Behl, M., Dhashmana, K., Sakhuja, D., Ghai, H., Sharma, N., Meena, K.R., Bhatt,
922 A.K., Bhatia, R.K., 2023. Non-food crops derived lignocellulose biorefinery for sustainable
923 production of biomaterials, biochemicals and bioenergy: A review on trends and techniques.
924 Ind. Crop Prod. 204, 117220. <http://dx.doi.org/10.1016/j.indcrop.2023.117220>.

925 Reis, C.E.R., Libardi Junior, N., Bento, H.B.S., Carvalho, A.K.F.d., Vandenberghe, L.P.d.S.,
926 Soccol, C.R., Aminabhavi, T.M., Chandel, A.K., 2023. Process strategies to reduce cellulase
927 enzyme loading for renewable sugar production in biorefineries. Chem. Eng. J. 451, 138690.
928 <http://dx.doi.org/10.1016/j.cej.2022.138690>.

929 Santos, P.H.A.D., Pereira, M.G., Trindade, R.d.S., Cunha, K.S.d., Entringer, G.C., Vettorazzi,
930 J.C.F., 2014. Agronomic performance of super-sweet corn genotypes in the north of Rio de
931 Janeiro. Crop Breed Appl. Biotechnol. 14, 8-14. [https://doi.org/10.1590/S1984-](https://doi.org/10.1590/S1984-70332014000100002)
932 [70332014000100002](https://doi.org/10.1590/S1984-70332014000100002)

933 Scordia, D., Cosentino, S.L., Jeffries, T.W., 2013. Enzymatic hydrolysis, simultaneous
934 saccharification and ethanol fermentation of oxalic acid pretreated giant reed (*Arundo donax*
935 L.). Ind. Crop Prod. 49, 392-399. <http://dx.doi.org/10.1016/j.indcrop.2013.05.031>.

936 Singh, N., Gupta, R.P., Puri, S.K., Mathur, A.S., 2021. Bioethanol production from pretreated
937 whole slurry rice straw by thermophilic co-culture. *Fuel* 301, 121074.
938 <http://dx.doi.org/10.1016/j.fuel.2021.121074>.

939 Unrean, P., Khajeeram, S., 2015. Model-based optimization of *Scheffersomyces stipitis* and
940 *Saccharomyces cerevisiae* co-culture for efficient lignocellulosic ethanol production.
941 *Bioresour. Bioprocess* 2, 41. <http://dx.doi.org/10.1186/s40643-015-0069-1>.

942 Wang, L., York, S.W., Ingram, L.O., Shanmugam, K.T., 2019. Simultaneous fermentation of
943 biomass-derived sugars to ethanol by a co-culture of an engineered *Escherichia coli* and
944 *Saccharomyces cerevisiae*. *Bioresour. Technol.* 273, 269-276.
945 <http://dx.doi.org/10.1016/j.biortech.2018.11.016>.

946 Wang, S., Sun, X., Yuan, Q., 2018. Strategies for enhancing microbial tolerance to inhibitors for
947 biofuel production: A review. *Bioresour. Technol.* 258, 302-309.
948 <http://dx.doi.org/10.1016/j.biortech.2018.03.064>.

949 Wang, Z.C., He, X.J., Yan, L.M., Wang, J.P., Hu, X.L., Sun, Q., Zhang, H.R., 2020. Enhancing
950 enzymatic hydrolysis of corn stover by twin-screw extrusion pretreatment. *Ind. Crop Prod.* 143,
951 111960. <http://dx.doi.org/10.1016/j.indcrop.2019.111960>.

952 Wojcieszak, D., Przybyl, J., Ratajczak, I., Golinski, P., Janczak, D., Waskiewicz, A., Szentner, K.,
953 Wozniak, M., 2020. Chemical composition of maize stover fraction versus methane yield and
954 energy value in fermentation process. *Energy* 198, 117258.
955 <http://dx.doi.org/10.1016/j.energy.2020.117258>.

956 Zabed, H., Boyce, A., Faruq, G., Sahu, J., 2016a. A comparative evaluation of agronomic
957 performance and kernel composition of normal and high sugary corn genotypes (*Zea mays* L.)
958 grown for dry-grind ethanol production. *Ind. Crop Prod.* 94, 9-19.
959 <http://dx.doi.org/10.1016/j.indcrop.2016.08.026>.

960 Zabed, H., Faruq, G., Sahu, J., Boyce, A., Ganesan, P., 2016b. A comparative study on normal and
961 high sugary corn genotypes for evaluating enzyme consumption during dry-grind ethanol
962 production. *Chem. Eng. J.* 287, 691-703. <https://doi.org/10.1016/j.cej.2015.11.082>.

963 Zabed, H., Sahu, J.N., Suely, A., Boyce, A.N., Faruq, G., 2017. Bioethanol production from
964 renewable sources: Current perspectives and technological progress. *Renew. Sust. Energ. Rev.*
965 71, 475-501. <http://dx.doi.org/10.1016/j.rser.2016.12.076>.

966 Zabed, H.M., Akter, S., Dar, M.A., Tuly, J.A., Kumar Aswathi, M., Yun, J., Li, J., Qi, X., 2023a.
967 Enhanced fermentable sugar production in lignocellulosic biorefinery by exploring a novel corn
968 stover and configuring high-solid pretreatment conditions. *Bioresour. Technol.* 386, 129498.
969 <http://dx.doi.org/10.1016/j.biortech.2023.129498>.

970 Zabed, H.M., Akter, S., Yun, J., Zhang, G., Zhao, M., Mofijur, M., Awasthi, M.K., Kalam, M.A.,
971 Ragauskas, A., Qi, X., 2023b. Towards the sustainable conversion of corn stover into bioenergy
972 and bioproducts through biochemical route: Technical, economic and strategic perspectives. *J.*
973 *Clean Prod.* 400, 136699. <http://dx.doi.org/10.1016/j.jclepro.2023.136699>.

974 Zabed, H.M., Akter, S., Yun, J., Zhang, G., Awad, F.N., Qi, X., Sahu, J.N., 2019. Recent advances
975 in biological pretreatment of microalgae and lignocellulosic biomass for biofuel production.
976 *Renew. Sust. Energ. Rev.* 105, 105-128. <http://dx.doi.org/10.1016/j.rser.2019.01.048>.

977 Zhai, R., Hu, J., Saddler, J.N., 2018. Minimizing cellulase inhibition of whole slurry biomass
978 hydrolysis through the addition of carbocation scavengers during acid-catalyzed pretreatment.
979 *Bioresour. Technol.* 258, 12-17. <http://dx.doi.org/10.1016/j.biortech.2018.02.124>.

980 Zhang, B., Li, J., Liu, X., Bao, J., 2022. Continuous simultaneous saccharification and co-
981 fermentation (SSCF) for cellulosic L-lactic acid production. *Ind. Crop Prod.* 187, 115527.
982 <http://dx.doi.org/10.1016/j.indcrop.2022.115527>.

983 Zhang, H., Zhang, R., Song, Y., Miu, X., Zhang, Q., Qu, J., Sun, Y., 2023. Enhanced enzymatic
984 saccharification and ethanol production of corn stover via pretreatment with urea and steam
985 explosion. *Bioresour. Technol.* 376, 128856. <http://dx.doi.org/10.1016/j.biortech.2023.128856>.

986 Zhu, J.-Q., Zong, Q.-J., Li, W.-C., Chai, M.-Z., Xu, T., Liu, H., Fan, H., Li, B.-Z., Yuan, Y.-J.,
987 2020. Temperature profiled simultaneous saccharification and co-fermentation of corn stover
988 increases ethanol production at high solid loading. *Energy Convers. Manage.* 205, 112344.
989 <https://doi.org/10.1016/j.enconman.2019.112344>.

990

991 **Table**

992

993 **Table 1.**

994 Composition of pretreated slurry and hydrolysate slurry obtained.

Parameters (g/L)	Pretreated slurry	Hydrolysate slurry
Glucose	31.26±0.43	86.67±1.1
Fructose	20.15±1.8	20.18±1.83
Xylose	25.3±1.2	29.59±1.92
Arabinose	2.98±0.15	3.24±0.13
Galactose	0.84±0.07	0.88±0.07
Sucrose	2.64±0.12	2.56±0.09
Total sugars	83.19±0.91	143.12±1.51
Acetate	3.73±0.52	3.73±0.52
5'-hydroxymethylfurfural	0.88±0.03	0.91±0.06
Furfural	0.81±0.02	0.82±0.02
total phenol content	3.11±0.03	3.21±0.06
Cellulose	56.53±1.66	3.17±0.32
Hemicellulose	5.49±0.78	1.26±0.28
Lignin	12.56±0.48	12.02±0.42

995

996

997

998

999

1000

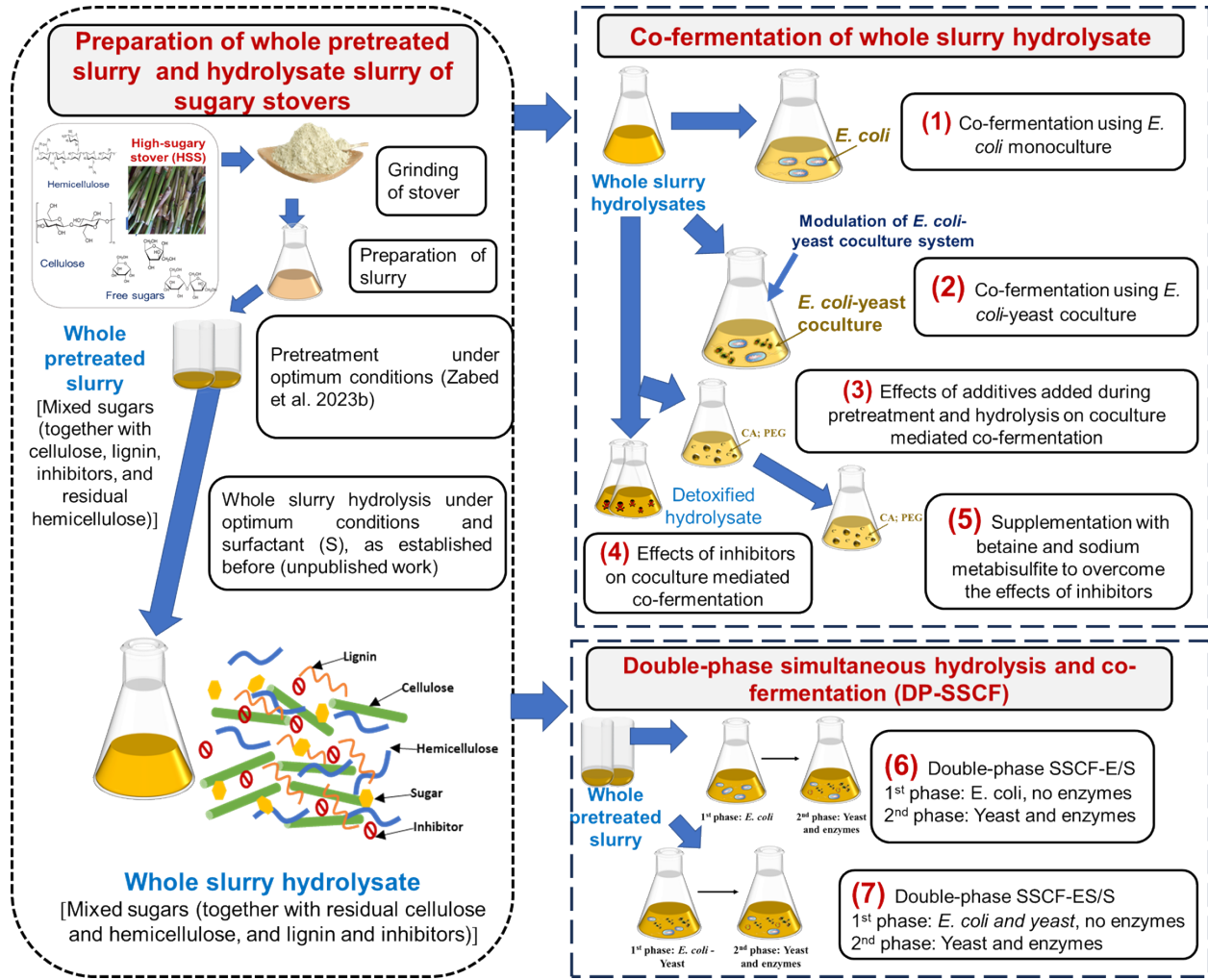
1001

1002

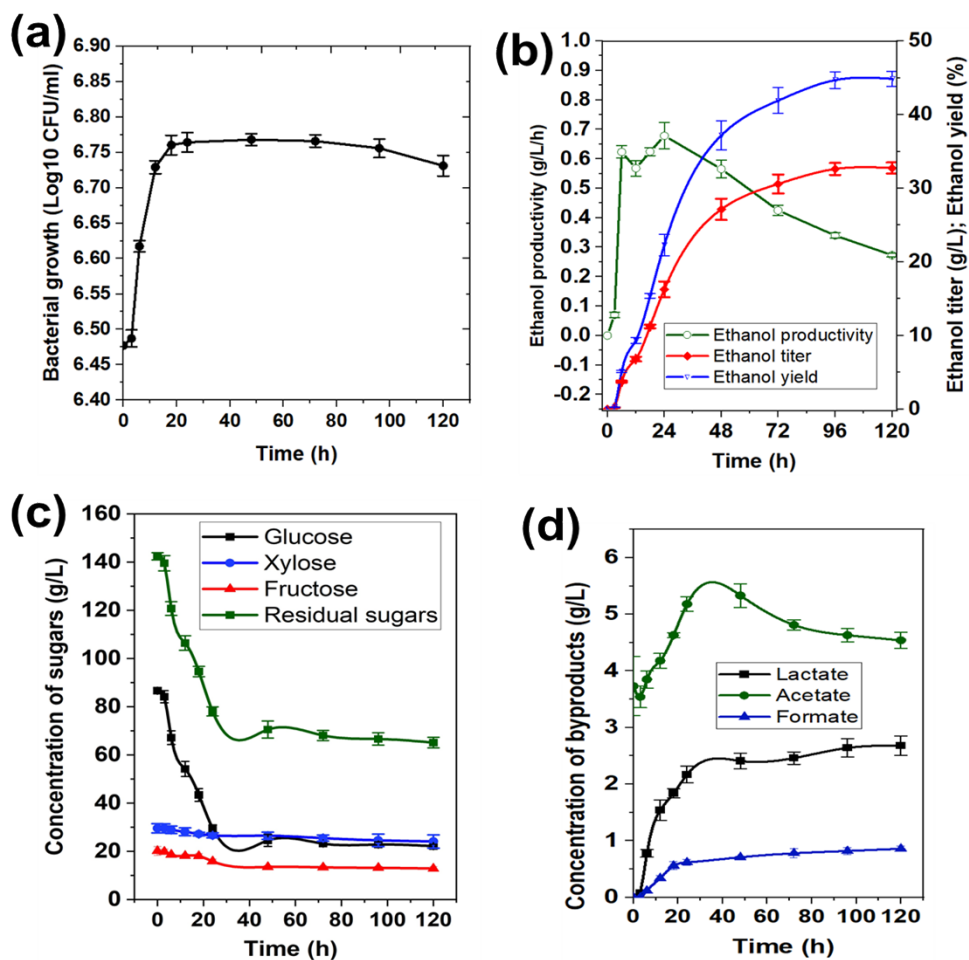
1003

1004

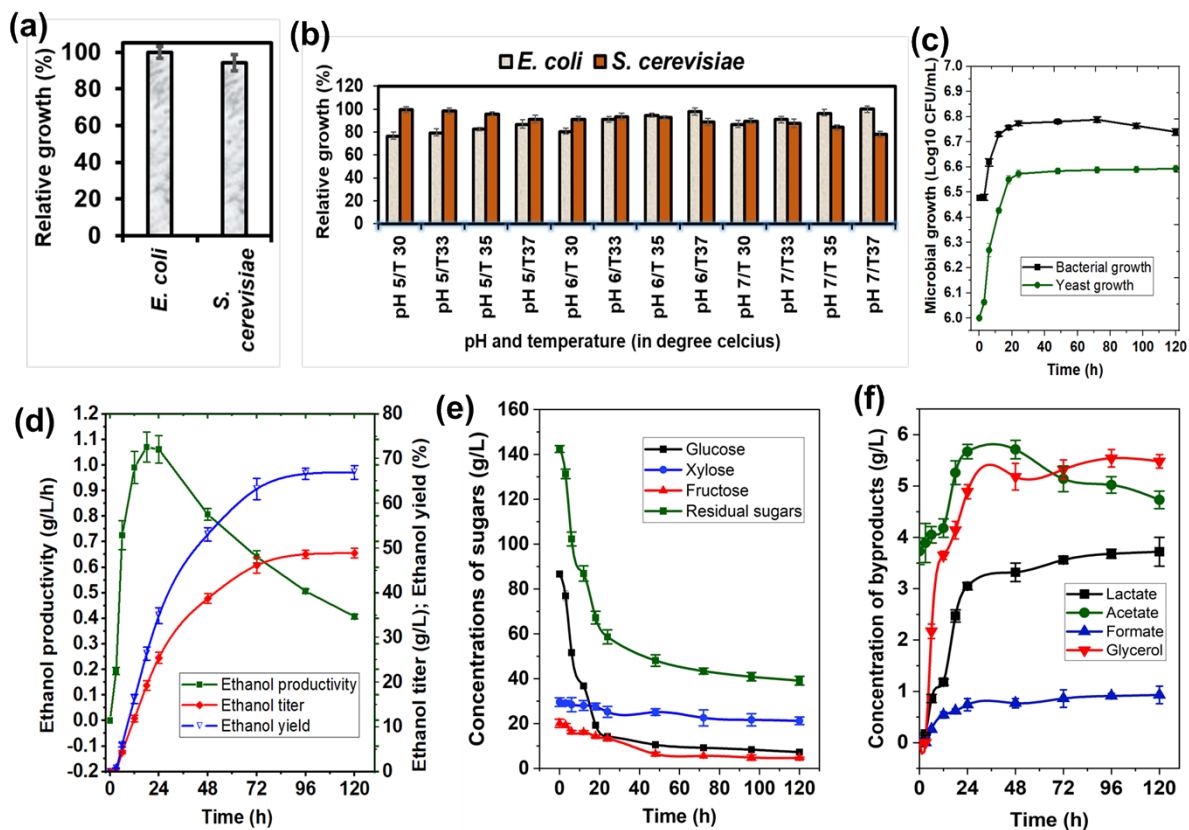
1005



1009 **Fig. 1.** Schematic diagram of the work design and flow of this study.



1012
 1013 **Fig. 2.** Co-fermentation of mixed sugars present in the undetoxified whole slurry hydrolysate
 1014 (SHCF) by *E. coli* monoculture: (a) bacterial growth; (b) ethanol production over time; (c) sugar
 1015 consumption during co-fermentation; and (d) byproduct generation during co-fermentation.
 1016
 1017



1018

1019 **Fig. 3.** Modulation of *E. coli*-*S. cerevisiae* coculture and coculture-mediated SHCF of hydrolysate:

1020 (a) growth of *S. cerevisiae* and *E. coli* in the modified LB medium relative to the growth in the

1021 standard medium (YPD broth and LB medium, respectively); (b) growth of *S. cerevisiae* and *E.*

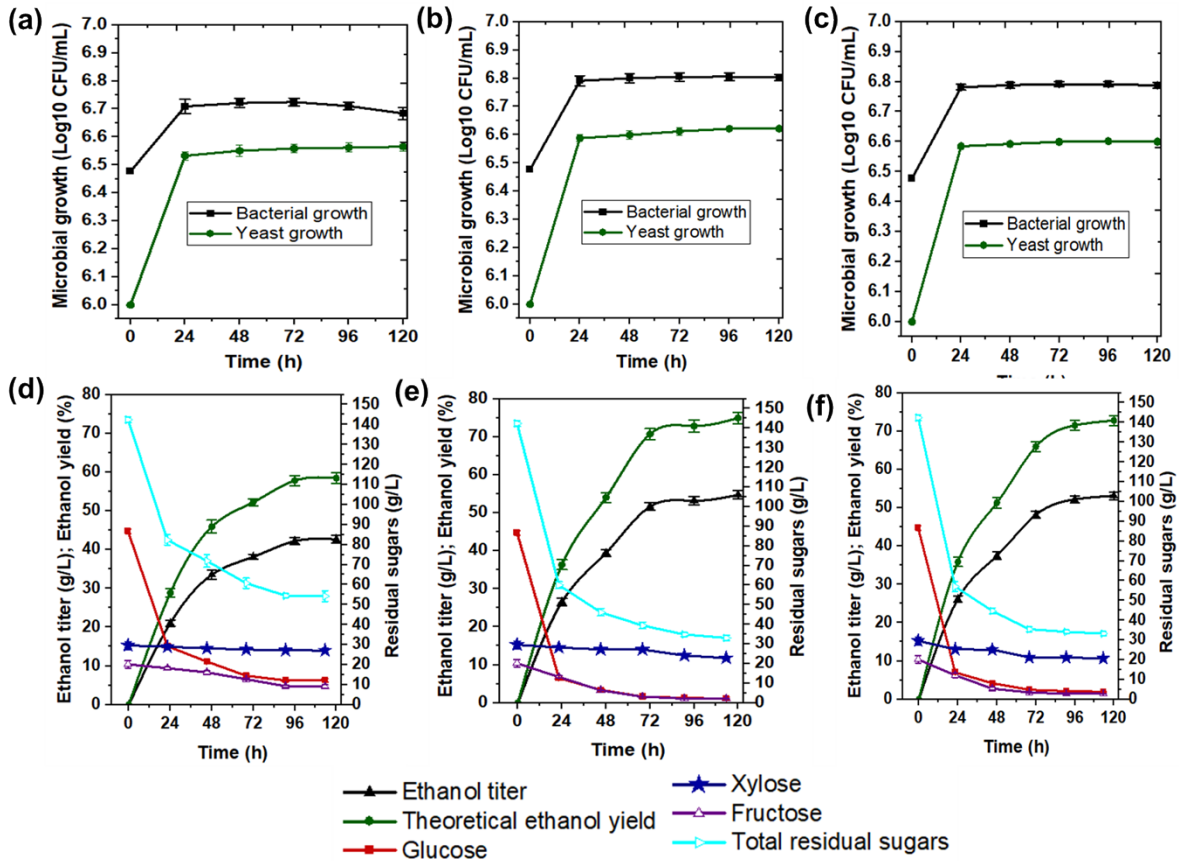
1022 *coli* in coculture system in modified LB medium under various pH and temperature conditions; (c)

1023 microbial growth over time during coculture-mediated SHCF; (d) ethanol production over time

1024 during coculture-mediated SHCF; (e) sugar consumption over time during coculture-mediated

1025 SHCF; and (f) byproduct generation over time during coculture-mediated SHCF.

1026



1027

1028 **Fig. 4.** Impacts of additives and detoxification on the performance of SHCF by *E. coli-S. cerevisiae*

1029 coculture system. (a and d) SHCF of undetoxified hydrolysate obtained without additives (synergic

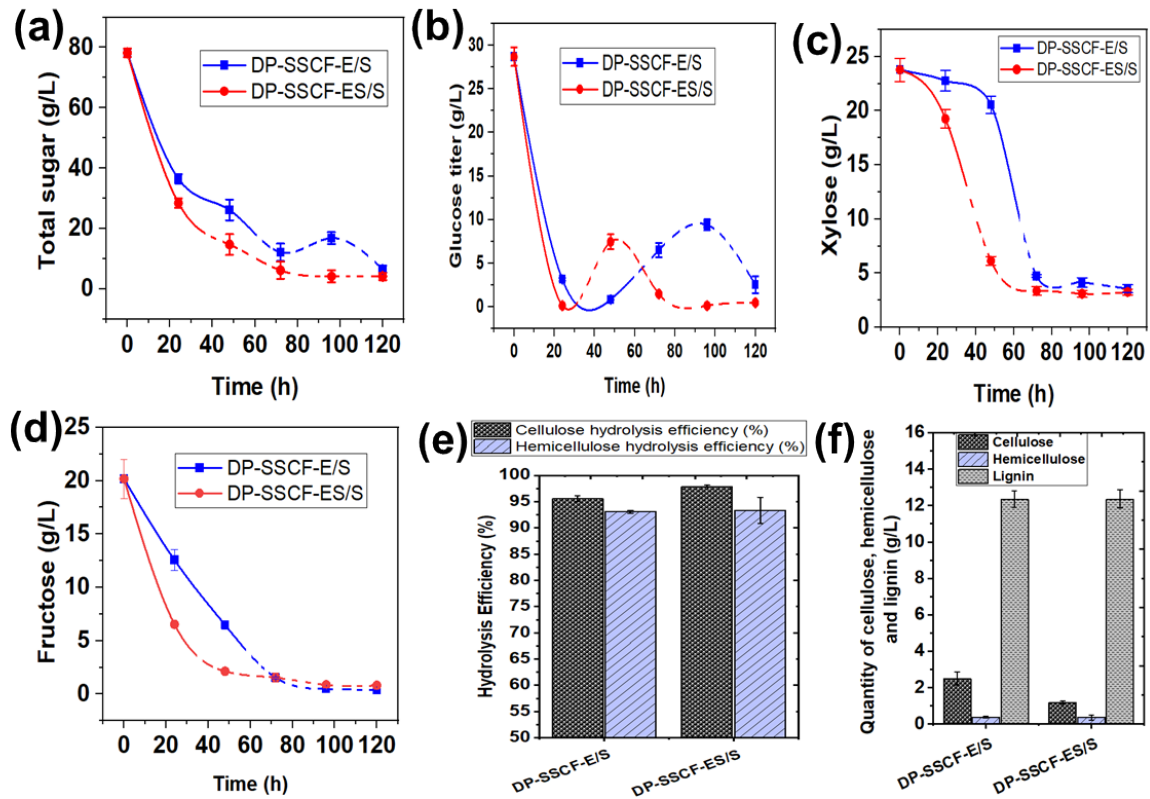
1030 acid during pretreatment and polyethylene glycol during hydrolysis); (b and e) SHCF of detoxified

1031 hydrolysate obtained without additives; and (c and f) SHCF of undetoxified hydrolysate obtained

1032 with additives, supplementation with betaine and sodium metabisulfite during fermentation.

1033

1034



1035

1036

1037

1038

1039

1040

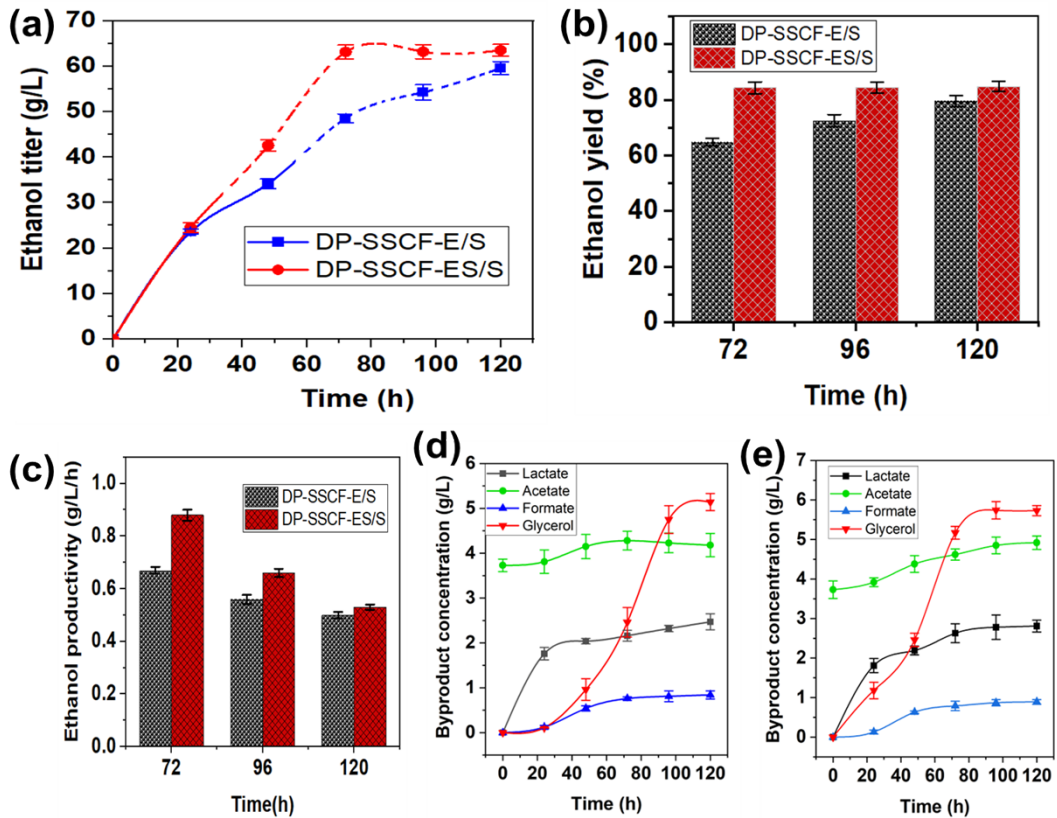
1041

1042

1043

1044

Fig. 5. Sugar consumption and hydrolysis of cellulose and hemicellulose during DP-SSCF under two different configurations, namely DP-SSCF-E/S (*E. coli* in the first phase and *S. cerevisiae* in the second phase) and DP-SSCF-ES/S (*E. coli*-*S. cerevisiae* coculture in the first phase and *S. cerevisiae* in the second phase). (a) Total sugar consumption; (b) glucose consumption; (c) xylose consumption; (d) fructose consumption; (e) cellulose and hemicellulose hydrolysis efficiency; and (f) residual lignocellulose content in the solid fraction at the end of DP-SSCF. The solid lines indicate the first phase of the respective configuration of DP-SSCF, while the dashed lines denote the second phase.



1045
 1046 **Fig. 6.** Ethanol and byproduct production during DP-SSCF under two different configurations,
 1047 namely DP-SSCF-E/S (*E. coli* in the first phase and *S. cerevisiae* in the second phase) and DP-
 1048 SSCF-ES/S (*E. coli*-*S. cerevisiae* coculture in the first phase and *S. cerevisiae* in the second phase).
 1049 (a) ethanol titer over time; (b) ethanol yield after 72-96 h; (c) ethanol productivity after 72-96 h;
 1050 (d) byproduct generation during DP-SSCF-E/S; and (e) byproduct generation during DP-SSCF-
 1051 ES/S. The solid lines indicate the first phase of the respective configuration of DP-SSCF, while
 1052 the dashed lines denote the second phase.

1053
 1054
 1055